Published in final edited form as:
Exp Neurol. 2013 November ; 249: 59–73. doi:10.1016/j.expneurol.2013.08.009.

Dorsal column sensory axons degenerate due to impaired microvascular perfusion after spinal cord injury in rats

Johongir M. Muradov[1,2], **Eric E. Ewan**[1,2], and **Theo Hagg**[1,2,3]

[1]Kentucky Spinal Cord Injury Research Center, University of Louisville, Kentucky 40292

[2]Department of Neurological Surgery, University of Louisville, Kentucky 40292

[3]Department of Pharmacology and Toxicology, University of Louisville, Kentucky 40292

Abstract

The mechanisms contributing to axon loss after spinal cord injury (SCI) are largely unknown but may involve microvascular loss as we have previously suggested. Here, we used a mild contusive injury (120 kdyn IH impactor) at T9 in rats focusing on ascending primary sensory dorsal column axons, anterogradely traced from the sciatic nerves. The injury caused a rapid and progressive loss of dorsal column microvasculature and oligodendrocytes at the injury site and penumbra and a ~70% loss of the sensory axons, by 24 hours. To model the microvascular loss, focal ischemia of the T9 dorsal columns was achieved via phototoxic activation of intravenously injected rose bengal. This caused an ~53% loss of sensory axons and an ~80% loss of dorsal column oligodendrocytes by 24 hours. Axon loss correlated with the extent and axial length of microvessel and oligodendrocyte loss along the dorsal column. To determine if oligodendrocyte loss contributes to axon loss, the glial toxin ethidium bromide (EB; 0.3 μg/μl) was microinjected into the T9 dorsal columns, and resulted in an ~88% loss of dorsal column oligodendrocytes and an ~56% loss of sensory axons after 72 hours. EB also caused an ~72% loss of microvessels. Lower concentrations of EB resulted in less axon, oligodendrocyte and microvessel loss, which were highly correlated ($R^2 = 0.81$). These data suggest that focal spinal cord ischemia causes both oligodendrocyte and axon degeneration, which are perhaps linked. Importantly, they highlight the need of limiting the penumbral spread of ischemia and oligodendrocyte loss after SCI in order to protect axons.

Keywords

axonal degeneration; blood flow; capillaries; contusion; ischemia; oligodendrocytes; spinal cord injury

Address for correspondence. Dr. Theo Hagg, Kentucky Spinal Cord Injury Research Center, 511 South Floyd Street, MDR, Building, Room 616, Louisville, KY 40292. theo.hagg@louisville.edu. Phone 502-852-8058, Fax 502-852-5148.

AUTHOR DISCLOSURE STATEMENT

No competing financial interests exist.

Introduction

Axonal protection is crucial for functional recovery after SCI, as residual neurological function may persist with survival of as few as 10% of axons (Fehlings and Tator, 1995). Axonal dysfunction and damage occurs immediately after SCI with complete loss of electrical conduction (James et al., 2011, Misgeld et al., 2007). The primary injury results in shear stress causing direct disruption of blood vessels and axons (Maikos et al., 2008). Subsequent secondary events such as microvascular dysfunction and loss, excitotoxicity and inflammation are thought to contribute to further tissue degeneration and functional deficits (Benton and Hagg, 2011, Cao et al., 2005, Donnelly and Popovich, 2008, Ek et al., 2010, Fassbender et al., 2011). In particular, microvascular spasm and subsequent ischemia contributes to neurodegeneration after compressive and contusive SCI (Anthes et al., 1995, Muradov and Hagg, 2013, Rivlin and Tator, 1978, Tator and Koyanagi, 1997). Direct impact to the spinal cord (Alford et al., 2011), release of vasoactive substances (Osterholm and Mathews, 1972), and hemorrhage (Guha et al., 1989, Mautes et al., 2000, Rosenberg et al., 2005) all contribute to the initiation and maintenance of reduced or absent perfusion, resulting in ischemia after SCI.

Our previous studies suggested that loss of microvessels at the injury epicenter might contribute to the loss of axons of passage. For example, intrathecal infusion of a protein tyrosine phosphatase inhibitor after a mild contusive SCI in rats that focuses the injury on the dorsal columns rescues ascending primary dorsal column sensory axons as well as the surrounding microvessels and tissue (Nakashima et al., 2008). Thus, endothelial cell loss might be one of the primary causes of subsequent axon degeneration and their rescue essential for neuroprotection. In fact, we have shown that treatment with intravenous angiopoietin-1, which only binds to the endothelial selective receptor Tie2, rescues tissue and function in mice (Han et al., 2010). However, that study did not analyze axonal projections and it remains unclear whether and how microvascular dysfunction might cause axonal degeneration. We have shown that contusions cause immediate loss of microvascular perfusion, with reperfusion around 6 hours and loss between 24 and 48 hours after contusive SCI (Muradov and Hagg, 2013). However, whether axonal degeneration occurs in concert with any of these microvascular deficits is unknown because the earliest time point we assessed sensory axon degeneration is at 3 days (Baker and Hagg, 2005). Understanding the timing and events leading to axonal damage and identification of the role of microvascular ischemia will help to develop treatments to protect axons after SCI.

Normal activity of axons depends on structural and functional integrity of the neurovascular unit which includes endothelial, glial and neuronal elements (Nave and Trapp, 2008). Axons are especially vulnerable to ischemic injury, which disrupts oxygen and glucose supply after SCI, due to their constant energy demands and absence of intrinsic energy reserves (Stys, 2004). Oligodendrocytes have been recognized as important for transporting energy substrates to axons (Fünfschilling et al., 2012). Therefore, oligodendrocyte cell loss as seen after contusive SCI (Almad et al., 2011, Frei et al., 2000) might compromise axonal function and survival.

The current study sought to understand the relationship between axon, microvascular, and oligodendrocyte loss after SCI using contusive, purely ischemic or gliotoxic injuries in rats, focusing on the primary ascending sensory axons of the dorsal column that project from the sciatic nerve to the nucleus gracilis in the medulla.

Material and methods

Animals

A total of 108 female Sprague Dawley rats were used (180 – 220 g; Harlan; Table 1). All invasive and animal care procedures adhered to the guidelines of the National Institutes of Health and were done with approval of the University of Louisville Institutional Animal Care and Use Committee. Animals were allowed to habituate to their cages for at least 48 hours after arrival and had free access to food and water.

Surgical procedures and postoperative care

All surgical procedures were performed with the aid of a Wild M695 motorized surgical microscope using the following standardized protocol. Deep anesthesia was achieved with an intramuscular injection of 3.3 ml/kg mixture containing 25 mg/ml ketamine hydrochloride (500 mg/ml, Hospira, Lake Forest, IL), 1.2 mg/ml acepromazine maleate (10 mg/ml, ButlerSchein, Dublin, OH), and 0.25 mg/ml xylazine (20 mg/ml, Akorn, Decantur, IL) in 13.3 ml of 0.9% saline. Protective ointment (Rugby Laboratories, Duluth, GA) was placed on the eyes to prevent corneal dehydration and injury and 5 ml of saline injected subcutaneously to prevent dehydration. Rats were placed on a water-circulating heating pad (Gaymar Industries, Orchard Park, NY) during surgery. After each procedure the surgical site was thoroughly rinsed with saline, the underlying soft tissue sutured with 5.0 silk, the skin closed with 9 mm metal clips (Braintree, ACS-cs, Braintree, MA), and Bacitracin ointment (Qualitest Pharmaceuticals, Huntsville, AL) applied to the incision cite. Postoperatively, an additional 5 ml of saline was injected to prevent dehydration and 0.1 ml of a 100 μg/ml stock solution of gentamicin (ButlerSchein, Dublin, OH) was injected intramuscularly to prevent infections; this dose of gentamicin was also administered 48 and 96hr postoperatively. Postoperative analgesia was achieved with 0.1 ml of 0.02% buprenorphine (Reckitt Benckiser Pharm., Richmond, VA) administered intramuscularly after surgery as well as every 12 hours for 48 hours. Rats recovered overnight on a water-circulating heating pad at 37°C, and afterwards their bladders were manually expressed twice a day until euthanasia or when spontaneous voiding recovered, whichever came first.

Spinal cord contusion and transection

A dorsal skin incision was made and soft tissue dissection done at the T8-T10 level. Laminectomy was performed after stabilizing T9 vertebra in a frame with steel clamps inserted under the transverse processes. For contusion injuries, an Infinite Horizons impactor (Precision Systems and Instrumentation, Lexington, KY) set at 120 kdyn with a 2.5 mm diameter impactor tip placed 5 mm above the intact dura before the contusion, was used. Sham operated animals received a laminectomy only. For transection injuries, the dura was opened and the dorsal part of the spinal cord was transected using the LISA-Vibraknife to the depth of 2 mm (Shields et al., 2008). Bleeding was stopped by hemostatic gelatin sponge (Gelfoam, Pharmacia & Upjohn Co, NY).

Rose bengal phototoxic injury

Phototoxic ischemia to the dorsal spinal cord was induced as previously described (Bunge et al., 1994). Briefly, the right external jugular vein was exposed by blunt dissection after a skin incision in the lateral cervical area. Two ligatures were placed around the vein and the upper ligature was loosely tightened to prevent blood flow. A small cut was made between the ligatures and custom made catheter pulled thinner over a flame from 1.2 mm diameter polyurethane catheter (cat # 72–4431; Harvard Apparatus, Holliston, MA) was inserted into the jugular vein over 10–12 mm. Afterwards, the lower ligature was tightened to fix the catheter in place. After exposure of the spinal cord at T9 by a laminectomy, 300 μl of 7.5

mg/ml (10 mg/kg) rose bengal (cat # 330000; Sigma, St. Louis, MO) solution was slowly injected intravenously through the jugular catheter over one minute. Two minutes after the injection the dorsal surface of the spinal cord was exposed for 2 minutes to a beam of 2 mm diameter green laser with 5 mw 532 nm Laser pointer (Amazon ID H8-8PBG-SC80) placed 10 cm above cord through the intact dura. Afterwards, the jugular catheter was removed and vein ligated to occlude the puncture point. Sham operated animals only received a laminectomy.

Intraspinal ethidium bromide injections

We used the gliotoxin EB to focally eliminate oligodendrocytes in the dorsal column (Blakemore, 1982). The spinal cord at T9 was exposed as previously described. The dura was carefully opened using fine forceps and two midline injections of EB (0.01 – 0.3 mg/ml, dissolved in saline) or saline spaced 1.5 mm apart were administered using custom-pulled glass micropipettes (30 – 40 μm diameter at their tips) attached to a Parker picospritzer. For each injection site the micropipette was first lowered 0.7 mm below the dorsal surface of the spinal cord and after 1 minute, 0.5 μl was injected. Three minutes later the micropipette was raised 0.3 mm (0.4 mm below the surface) and a minute later a second 0.5 μl was injected. After another 3 minutes the micropipette was retracted from the spinal cord. One group of animals received a single midline injection 0.7 and 0.4 mm below the dorsal surface at T9.

Locomotor testing

Behavioral tests were conducted weekly from 7 to 35 days after EB or saline injection. Rats were acclimatized to the being handled (gentled) and to the equipment and baseline values determined before the surgery. Open field overground locomotor function was assessed using the Basso-Beattie-Breshnahan (BBB) scale (Basso et al., 1996). Briefly, rats were allowed to walk in a 85 cm diameter open field (circular tub) while two certified examiners scored locomotor performance over 4 minutes. Afterwards, rats were also tested on a grid walk test, which is dependent on the dorsal column (Nakashima et al., 2008). During testing, rats walk voluntarily for a total of 90 seconds over a maximum of 150 seconds on a 114 cm × 114 cm inch grid with 3.8 cm holes (plastic-coated chain-link fence) suspended on the corners by metal rods. Two observers positioned on opposite sides of the grid record the number of hind limb footfalls, while a third observer records the time of voluntary walking (90 seconds) and total time of each test.

Dorsal column primary sensory axon tracing

Dorsal column sensory projections from the sciatic nerve to the nucleus gracilis in the medualla were traced with choleratoxin B (CTB) (Baker and Hagg, 2005, Baker et al., 2007, Nakashima et al., 2008). Therefore both sciatic nerves were injected as previously described (Baker et al., 2007) with minor modifications. Briefly, after a small incision on the lateral thigh area on each side and soft tissue dissection, the sciatic nerves were identified. A ligature was loosely placed on the nerve 5–8 mm proximal to the split of the tibial and fibular nerves, and a segment of the nerve crushed with a plain fine forceps to enhance tracer uptake. A 30 gauge needle connected through a polyurethane catheter (Cat # 72–4431; Harvard Apparatus, Holston, MA) to a Hamilton syringe was inserted into the crushed segment through the inside of the nerve and through the loose ligature, which was then tightened to secure the needle in place. Two μl of 1% cholera toxin B (CTB; List Biologicals, Campbell CA) solution was then slowly injected over 1 minute and the needle left in place for an additional 2 minutes. The needle was then withdrawn from the nerve and the ligature removed.

Histological procedures: axonal projections

Prior to euthanasia animals were anesthetized and the left jugular vein was exposed. Two hundred μg of texas red-conjugated lycopersicon esculentum (LEA; Cat#TL-1176; Vector Laboratories, Burlingame, CA) in a volume of 200 μl was slowly injected intravenously through a 26 gauge needle over 1 minute and allowed to circulate for 20 minutes. LEA binds to and labels endothelial cells and therefore identifies perfused microvessels with an endothelial lining (Benton et al., 2008, Han et al., 2010). Afterwards, rats were perfused with 200 ml ice-cold 0.1 M phosphate buffered saline (PBS) followed by 200 ml 4% paraformaldehyde (Cat #19210; Sigma, St. Louis, MO) in phosphate buffer. The brain and spinal cord were dissected and postfixed in 4% paraformaldehyde overnight, and were then cryoprotected in 30% sucrose until they sank.

To reveal traced axon terminals, 30 μm thick sagittal sections from the medulla were cut using a freezing sliding microtome and collected and stored in phosphate buffer based 0.12 M Millonig's solution. Horizontal sections through the lumbar spinal cord were used to confirm the quality of anterograde tracing of the uninjured sensory afferents and motor neurons from the sciatic nerves. CTB immunostaining was performed on free-floating sections. Sections were incubated for 30 min in 0.3% H_2O_2 (Cat # HX0635-1; EMD Millipore, Philadelphia, PA), then washed 3 × 10 min in PBS and then incubated in PBS containing 0.25% Triton with 5% normal rabbit serum to reduce non-specific protein binding including that of secondary antibodies. Afterwards, sections were incubated overnight in cold room goat-anti CTB (Cat# 703; 1:80,000; List Biologicals) in PBS-0.25% Triton with 5% normal rabbit serum. The next day sections were washed 3 × 10 min in PBS, and then incubated at room temperature for 1 hour in rabbit anti-goat IgG (Cat# BA5000; 1:300; Vector Laboratories, Burlingame, CA) in PBS-0.25% Triton with 5% normal rabbit serum. Sections were then washed 3 × 10 min in PBS followed by incubation for 1 hr in avidin-biotin complex kit (Cat #PK6100; 1:600; ABC Elite; Vector) in 2% NaCl to suppress non-specific staining. Sections were washed 3 × 10 min in PBS and then incubated for 10 minutes in diaminobenzidine (DAB) solution that was prepared fresh with 0.4 mg/ml DAB (Cat #D5637, Sigma, St. Louis, MO), 0.6 mg/ml ammonium nickel sulfate and 0.6 μl/ml of 0.3% H_2O_2 all dissolved in 0.05 M Tris HCl buffer. Afterward, slides were rinsed 3 × 10 min in PBS, 1 × 10 min in 0.1 M phosphate buffer and then mounted on 0.1 % gelatin-coated slides and allowed to dry overnight. The next day, the slides were dehydrated in a series of increasing concentrations of ethanol up to 100% followed by xylene, and then cover slipped in Permount (Cat# SP15–500, Fisher Scientific; Pittsburg, PA).

Histological procedures: injury site

To analyze the injury site, an 11 mm segment of spinal cord centered around the injury epicenter was collected and cast in Tissue Freezing Medium (TMF-5, Triangle Biomedical Sciences Inc., Durham, NC) and frozen at −20°C with other specimens of experiment. The block was cut using a cryostat in 20 μm transverse sections and every other section was collected on SuperFrost plus glass slides (VWR, Radnor, PA).).

For immunohistochemistry of the thoracic injury site every fifth transverse slide collected (i.e., spaced 200 μm apart along the spinal cord axis) was stained in order to quantify blood vessels and oligodendrocyte cell bodies along the length of the spinal cord. Slides were dried at 37°C for 60 min and freezing medium was removed with forceps. A border was drawn with a slide marker (Cat # 195500, RPI, Mount Prospect, IL). Slides were washed 3 × 10 min in PBS, were blocked in PBS-0.25% Triton with 5% normal donkey serum for 1 hour, and were then incubated overnight in the primary antibodies diluted in PBS-0.25% Triton with 5% normal donkey serum. The next day, slides were washed 3 × 10 min in PBS, incubated in secondary antibodies diluted in PBS for 1 hr, and then were washed 3 × 10 min

in PBS, 1 × 10 min in PB, and coverslipped with Fluoromount-G (Cat#0100-01; Southern Biotech, Birmingham, AL). Primary antibodies used were goat anti-texas red IgG (1:500, Cat SP-0602, Vector Laboratories; Burlingame, CA) to detect texas red conjugated LEA bound to endothelial cells in perfused blood vessels, mouse anti-rat RECA (1:1000; catalog #MCA970; Serotec, Raleigh, NC) to detect all endothelial cells, and mouse anti-APC (1:1000; Cat # OP80, Calbiochem, Billerica, MA) for oligodendrocytes. Secondary antibodies were Alexa 594-conjugated donkey anti-goat (1:200; Cat#A11058; Invitrogen, Grand Island, NY) or Alexa 488-conjugated donkey anti-mouse (1:200; Cat#A21202; Invitrogen), depending on the species of the primary antibody.

To reveal the extent of white matter damage along the length of the spinal cord, eriochrome cyanine (EC) staining of every fifth slide collected was used (Rabchevsky et al., 2001). Slides were dried and freezing medium removed as described above. Slides were immersed for 2 × 30 min in xylene, for 3 minutes each in 100%, 95%, 70%, and 50% ethanol, and then for 10 minutes in EC staining solution (2 ml of 10% $FeCl_3$ (cat # 157740; Sigma) and 40 ml of 0.2% EC (cat # 32752; Sigma) in 0.5% aqueous H_2SO_4 (cat # 339741; Sigma) brought to a final volume of 50 ml with ddH_2O). Tissue was then rinsed in ddH_2O and differentiated with 0.5% aqueous NH_4OH (cat # 221228; Sigma) for 30 seconds, and then immediately immersed in ddH_2O to terminate the reaction. Slides were dried overnight and after progressive dehydration in alcohol and immersing in xylene were coverslipped in Permount (SP15–500, Fisher Scientific, Pittsburg, PA).

Quantitative measurements

High resolution stitched (mosaic) images were taken of sections through the medullar region containing the nucleus gracilis or of whole transverse sections of the spinal cord. This was achieved with a DM 6000 Leica upright microscope with a 20× objective (for fluorescent images) and 10× objective (for bright field images) combined with Surveyor software (Objective Imaging, Cambridge, UK) and an Oasis Automation Controller (Objective Imaging, Cambridge, UK) driving a motorized stage.

ImageJ 1.45s software (Wayne Rasband, NIH, Bethesda, MD) was used to determine sparing of sensory axons projecting through the injury site to the medulla. Only rats with normal CTB staining of the lumbar enlargement were included for sensory axon analysis, since this ensures successful CTB uptake after sciatic injection. Each CTB+ area of the nucleus gracilis was circled and the area outside it was cleared. The picture was then transformed to an 8-bit image and the threshold of CTB+ staining manually adjusted to define the ratio of CTB+ pixels to the entire image area (including the cleared part). Sum of ratios of all sections of each animal were calculated and expressed as a percentage of sham. Left and right sides were combined for each animal.

Dorsal column microvessels at the injury site and penumbra were counted manually with a grid intersection method. Briefly, images were opened in Adobe Photoshop CS5 software (Adobe systems, San Jose, CA), rotated to the anatomical position and the dorsal column encircled. A grid with 100 μm cell sizes was placed over the dorsal columns with its bottom border placed on the central canal. Tube-structured LEA or RECA+ microvessels intersecting the horizontal or vertical lines were counted manually. APC+ oligodendrocytes were counted manually throughout the entire dorsal column. The injury epicenter was defined based on the sections with the lowest number of microvessels (contusion and rose bengal models) or oligodendrocytes (EB model). The averages of microvessel and oligodendrocyte quantity in three sequential sections (spaced 200 μm) at the epicenter as well as at mm distances rostral and caudal to it were calculated for each animal (Han et al., 2010). The length of microvessel or oligodendrocyte injury for each subject was defined as the area in which microvessels or oligodendrocytes were less than 33% of sham values.

In the group of animals with chronic injury, quantification of spared white matter was done using ImageJ 1.45s software (Wayne Rasband, NIH, Bethesda, MD). The dorsal column of EC-stained sections was encircled, a binary image created, and the percentage of stained pixels calculated. The section with the lowest percentage of EC area was defined as the epicenter. Averages of three sequential sections at the epicenter and at mm distances rostral and caudal were calculated for each animal.

Statistical analysis

All values are presented as group averages plus or minus SEM. Where indicated values were recalculated as a percentage of their sham operated control rats. In experiments with two groups the Student t-test was used to determine whether statistical differences existed. To compare more than two groups, one way ANOVA was performed. When more than one variable was compared we used two-way ANOVA or repeated measures ANOVA (behavioral tests). Post-hoc analyses were performed using Dunnett's test for multiple comparisons when determining differences from control, and Tukey's test for multiple comparisons when determining differences between experimental groups. Microsoft Excel 2010 (Microsoft Co., San Jose, CA) was used to collect and organize data and Prism 6 (GraphPad, La Jolla, CA) was used for statistical testing, with $p<0.05$ considered statistically significant.

Results

Axonal degeneration occurs within 24 hours following mild spinal cord injury

We have extensively used tracing to the medulla as a tool to define the extent of survival of ascending dorsal column primary sensory axons following contusions and treatments (Baker and Hagg, 2005, Baker et al., 2007). Sciatic injection of the anterograde tracer CTB results in tracing of only 10% of the projections to the nucleus gracilis by 24 hours, with robust and maximal tracing at 72 hours (Baker and Hagg, 2005). That method is therefore unable to assess axonal degeneration over times less than three days. Here, we first defined a tracing protocol which would enable us to better define when the degeneration occurs after a T9 contusion. No differences in CTB-traced projections to the nucleus gracilis was observed in sham animals 48 (Figure 1A) or 72 (not shown) hours after sciatic injection (Figure 2B; $p>0.05$), indicating that more than 85% of these sensory axonal projections are fully labeled between 24 and 48 hours. Compared to sham operated rats with a 48 hour tracing period (Figure 1A), rats that had received CTB injections 24 hours prior to a T9 transection of the dorsal spinal cord (Figure 1B), had 14 ± 3% of their projections in the nucleus gracilis (n=5; Figure 2C, $p<0.05$). This confirms that the amount of tracer reaching the medulla during the first 24 hours is minimal (Baker & Hagg 2005) and does not increase following axonal degeneration, giving us a tool to evaluate the survival of axons over the next 24 hours (for a total of 48 hours of tracing). After a 120 kdyn contusive SCI at T9, given 24 hours after tracer injection, the percentage of CTB+ projections was not significantly different whether tissue was collected at 24 hours (30 ± 4%; n=5; Figure 1C, 2C), 48 hours (21 ± 3%; n=4) or at 7 days (29 ± 1%; n=6) after SCI (all $p>0.05$). Therefore, essentially all sensory axon loss occurs within the first 24 hours after contusion. These values correspond well to our previous findings which used 72 hours of tracing prior to analysis at 7 days after mild contusions (Baker and Hagg, 2005), thus validating the new pre-injury tracing technique. The CTB values at 24 hours after the contusion were higher than after the transection (Figure 2C, $p<0.01$), indicating that at least ~20% of the axons remained intact.

Loss of dorsal column microvasculature occurs during the acute phase of contusive SCI

We next set out to determine whether microvessels would be lost within the first 24 hours after a contusive SCI, i.e., within a similar period as the sensory axons. We used the 120

kdyn injury at T9 because damage is predominantly seen in the dorsal columns and because 70% of the fibers are lost, enabling detection of increases as well as decreases in axonal survival. In sham-operated rats, dorsal column microvessels had a uniform distribution, as shown by LEA labeling in perfused microvessels and by the general endothelial cell marker RECA (Figure 3A,B). Early after contusion, fewer perfused LEA+ and RECA+ blood vessels were seen in the dorsal column and medial parts of the dorsal horns, indicative of a disruption of microvasculature and blood flow (Figure 3E). The more ventral parts of the cord were not affected (data not shown).

At the injury epicenter, the contusion decreased the total (RECA staining) and perfused (LEA staining) number of microvessels within the dorsal columns already at the earliest 3 hour time point (Figure 4A; $p<0.05$). Total and perfused microvessel numbers at the epicenter did not change significantly between 3, 6, and 12 hours after injury. At 12 hours only 19 ± 7% RECA+ and 5 ± 2% LEA+ microvessels remained present compared to sham (Figure 4A). In the injury penumbra at 1 mm rostral and caudal from the epicenter the number of perfused microvessels was also decreased by 3 hours (47 ± 9%; $p <0.05$ vs. sham) and progressed to even lower numbers at 12 hours (17 ± 4%; $p < 0.01$ vs. 3 hours; Figure 4B). The total number of microvessels (RECA) was not significantly decreased until 12 hours after contusion (39 ± 7 % of sham; $p<0.05$; Figure 4A), suggesting a progressive phase of endothelial cell death starting sometime after 3–6 hours. By and large, the number of LEA+ microvessels was lower than the total number indicating the presence of vasospasm in the surviving ones, most notably over the first 6 hours in the penumbra.

Loss of dorsal column oligodendrocytes occurs acutely after contusive SCI

Oligodendrocyte cell bodies were assessed in adjacent sections. In sham animals, APC+ dorsal column oligodendrocytes were distributed equally (Figure 3C). In the injured animals only some oligodendrocytes remained present, most evident in the rim of spared peripheral white matter (Figure 3F). Some areas of the adjacent dorsal horn gray matter were also devoid of oligodendrocytes. Interestingly, the APC+ cell bodies seemed to remain in areas of LEA+ perfused microvessels. Quantification revealed that the contusion caused a dramatic decrease to ~10% in dorsal column oligodendrocytes at the epicenter as early as 3 hours (11 ± 3 %), which remained decreased at 6 and 12 hours (13 ± 2 % and 9 ± 1 %, respectively; $p<0.05$; Figure 4C). In the injury penumbra, the number of APC+ oligodendrocytes was decreased by 3 hours after injury, albeit to a lesser extent than at the epicenter (46 ± 3%; $p <0.001$), with the greatest loss 12 hours after SCI (33 ± 2 % of Sham; $p<0.05$; Figure 4C). The number of oligodendrocytes at the injury epicenter correlated with number of LEA+ ($R^2=0.69$, $p<0.05$) and RECA + microvessels ($R^2=0.65$; $p <0.05$).

Phototoxic injury eliminates dorsal column microvessels

To model ischemia and microvessel loss observed after contusive SCI, we used the rose bengal-induced phototoxic vascular ischemic injury (Bunge et al., 1994) at T9. Twenty four hours following phototoxic injury there was an almost complete loss of LEA+ (perfused) and RECA+ microvessels in the dorsal column as well as in the adjacent grey matter (Figure 5E,F injured vs. A,B in sham). The depth of the injury seemed to be limited to the dorsal half of the thoracic spinal cord. At the injury epicenter only 6 ± 4% of total (RECA) and 7 ± 4% of perfused microvessels (LEA) were observed compared to sham (Figure 6; $p<0.01$). Total and perfused blood vessels in the rostral and caudal 1 mm penumbra were also significantly decreased compared to sham (RECA, 37 ± 12%, $p<0.05$ and LEA, 37 ± 12 %, $p<0.01$). At 2 mm rostral or caudal to the epicenter, the number of microvessels did not differ from sham (Figure 7A). The average length of ischemic injury along the spinal cord axis, defined as the sections in which less than 33% of dorsal column microvessels remained present, was 2.4 ± 0.5 mm for RECA and 2.1 ± 0.6 mm for LEA.

Axial length of ischemic injury correlates with dorsal column sensory axons loss

Similar to the 120 kdyn contusion injury, the phototoxic injury decreased the sensory projections to the nucleus gracilis by 24 hours compared to sham (Figure 5J vs. I). The percentage of CTB projections was decreased to 53 ± 6% of sham (Figure 6, $p<0.001$, which is significantly higher when compared to the contusion injury (30 ± 4%, $p<0.01$). There was no significant correlation between the loss of CTB+ axonal projections in the nucleus gracilis and microvessels at the epicenter (data not shown). However, the axon loss correlated well with the length of the ischemic injury (RECA, $R^2 = 0.67$, LEA, $R^2=0.80$; $p<0.05$; Figure 7B).

Ischemia causes acute dorsal column oligodendrocyte and myelin loss

The phototoxic ischemia injury caused a loss of APC+ oligodendrocyte cell bodies in the dorsal column after 24 hours. Similarly to the contusion injury, loss of oligodendrocytes was observed throughout the dorsal column at the injury epicenter (Figure 5G v.s C, sham), while in the penumbra more extensive damage is observed in the ventral portions of the dorsal column white matter. Many of the cell bodies seemed to be swollen and fragmented (Figure 5G, insets). The injury caused a decrease in the number of dorsal column APC+ oligodendrocytes at the injury epicenter (17 ± 5%, $p<0.05$, Figure 6) and the penumbra at 1 mm from the epicenter (37 ± 9%, $p<0.05$). Of note is that the number of oligodendrocytes was also significantly decreased at 2 mm from the epicenter (57 ± 8% of sham, $p<0.01$, Figure 7C) even though total and perfused microvessels were not significantly different from sham at this distance (Figure 7A). The number of oligodendrocytes at the epicenter correlated with axon loss ($R^2=0.86$; $p<0.05$). The average length of oligodendrocyte injury after phototoxic ischemia, defined as the area in which 33% of dorsal column oligodendrocytes remained, was 3.1 ± 0.5 mm. Similar to microvascular loss, the length of dorsal column oligodendrocytes injury correlated with axon loss (Figure 7D, $R^2=0.80$; $p < 0.05$). Interestingly, the phototoxic ischemia injury also caused loss of EC staining of myelin (Figure 5H vs. D, sham), which is not generally seen after contusion. The loss of myelin by EC staining overlapped with areas of loss of microvessels and oligodendrocytes. Quantification showed a decrease in dorsal column white matter at the epicenter (72 ± 6%; $p<0.05$; Figure 6). The length of myelin injury correlated with the loss of axons (Figure 7D, $p<0.05$). The values of dorsal column EC staining were higher than that of the APC+ oligodendrocytes, as expected for myelin, which degenerates over longer times.

The gliotoxin EB dose-dependently eliminates dorsal column oligodendrocytes and myelin

Microinjections of EB into the dorsal column at T9 were used to determine whether perhaps the glial injury after the contusive or ischemic injuries might contribute to the ascending sensory axon loss. Two EB injections spaced 1.5 mm apart caused an almost complete loss of APC+ cell bodies in the dorsal column by 3 days (Figure 8A vs. E). Damage from EB to oligodendrocytes was most concentrated near the midline of the dorsal column, and appeared in the form of an ellipse due to injecting at two depths per site (0.7 mm and 0.4 mm from the surface). The width of this ellipse was the greatest at epicenter, covering most all of the dorsal column, and gradually decreased in width away from the epicenter. In most cases the damage was restricted to the white matter, with occasional damage into the nearby edges of the dorsal and intermediate grey matter. In most all instances the dorsal column appeared swollen at the epicenter compared to Sham. Quantification showed that EB decreased dorsal column white matter oligodendrocytes in a dose- and distance-dependent manner ($p<0.0001$) 3 days after injection (Figure 9A). The number of dorsal column APC+ cell bodies at the injury site was significantly decreased compared to sham for rats given two intraspinal injections of 1 μl of 0.03 (47 ± 16% epicenter; $p < 0.05$), 0.1 (30 ± 10% epicenter; $p < 0.001$; (44 ± 12% penumbra; $p < 0.01$), and 0.3 μg/μl EB (12 ± 2% epicenter; $p < 0.0001$; 10 ± 5% penumbra; $p < 0.0001$; Figure 9A). The length of dorsal column

oligodendrocyte loss (less than 33% remaining in sections) was significantly different from sham only in rats receiving two injections of 0.3 μg/μl EB ($p<0.001$; Figure 9C). Oligodendrocyte loss should lead to myelin loss, and we therefore assessed myelin EC staining following EB. Of the concentrations assessed at 3 days post-injection, only 0.3 μg/μl EB significantly decreased dorsal column white matter compared to sham treatment and only at the epicenter (78 ± 5%, $p<0.01$; Figure 8B vs. F, Figure 10A). Myelin loss exhibited a similar elliptical shape as oligodendrocyte loss, except that at 3 days the width of myelin loss is less throughout the epicenter and penumbra, and is more focused near the midline, suggesting that midline oligodendrocytes may be lost first, with gradual loss occurring further from the midline. By 7 days the entire dorsal column is demyelinated (not shown). Dorsal column white matter sparing following EB injection was worse after 7 and 42 days, with 23 ± 9% and 30 ± 4% remaining, respectively, both of which were significantly different from the 3 day time point ($p<0.001$ and $p<0.01$ for 7 and 42 days, respectively; Figure 10B).

EB causes a loss of dorsal column sensory axons

To assess whether oligodendrocyte loss would be associated with sensory axon loss rats received two injections of EB spaced 1.5 mm apart into the dorsal column at T9. Of the concentrations assessed, only 0.3 μg/μl produced a significant decrease of sensory axons to 44 ± 10% of sham three days after administration ($p<0.05$; Figure 8I vs. J; Figure 11A). To determine if sensory axons continue to degenerate after 3 days, later time points after EB were also assessed. The extent of axon sparing was not significantly different from 3 days in separate groups of rats at 7 and 42 days after EB injection (21 ± 7% and 35± 11%, respectively; $p>0.05$; Figure 11B). This suggests that like contusive injury (Figure 2) most axon loss occurs acutely after EB injection.

EB also causes dorsal column microvessel loss

Given the tight relationship we found between ischemia and oligodendrocyte and axon loss in the other models, we assessed the effects of EB on microvessels. Surprisingly, EB caused a loss of total (RECA) and perfused (LEA) microvessels in the dorsal column by 3 days (Figure 8C and D vs G and H). The distribution of damaged microvessels had an an elliptical pattern and was very similar to that described for oligodendrocytes in adjacent sections, and with the dorsal and intermediate grey matter mostly being spared. The number of LEA+ microvessels was significantly decreased compared to sham animals only at 0.3 μg/μl EB (25 ± 2% epicenter; $p < 0.01$; 36 ± 9% penumbra; $p<0.05$; Figure 9B). Note that three days after EB administration RECA and LEA staining was in almost all cases identical, indicating that virtually all microvessels remaining were perfused; for this reason 3 day figures only show LEA quantification, but reflect RECA values as well. Similar to oligodendrocyte loss, the length of dorsal column blood vessel loss (less than 33% of Sham) was significantly different from sham only in rats receiving injections of 0.3 μg/μl EB at two sites along the spinal cord ($p<0.01$; Figure 9C). Loss of epicenter perfused blood vessels lasted at least 42 days, with LEA+ staining significantly decreased compared to SHAM at 3, 7 and 42 days after EB injection ($p<0.01$; Figure 9D). Similarly, total dorsal column blood vessels, assessed with RECA staining, were decreased 3 and 42 days after EB administration ($p<0.01$ and $p<0.05$ for 3 and 42 days, respectively; Figure 9D). Similar effects were observed at the epicenter of rats receiving a single injection of EB, with LEA but not RECA being significantly decreased 7 days after injection ($p<0.05$; Figure 9D). Differences in RECA and LEA staining 7d after EB (Figure 9D) likely reflect angiogenesis of non-perfused microvessels, highlighting the importance of using LEA to label perfused vessels (Benton et al. 2008; Han et al 2010).

Axon loss correlates with length of oligodendrocyte and microvessel loss

Across all concentrations of EB (0.03–0.3 μg/μl) the degree of oligodendrocyte and microvascular loss at the epicenter was highly correlated (R^2=0.81, p<0.0001; Figure 12A). In contrast, axon degeneration assessed by nucleus gracilis CTB+ staining correlated less with loss of epicenter oligodendrocyte (R^2=0.44, p<0.05; Figure 11B) and microvessels (R^2=0.29, p<0.05; Figure 12B). In fact, the correlation was due to the three rats receiving 0.3 μg/μl EB and was lost when they were removed (oligodendrocytes, R^2=0.04; microvessels, R^2=0.03; p>0.05). Interestingly, in the lower EB dose groups (0.01 – 0.1 μg/μl) oligodendrocyte and microvessel number remained highly correlated (R^2=0.70, p<0.01), indicating that some can die without affecting axon degeneration, and that their loss occurs independent of axon loss. However, similar to phototoxic ischemia, the length of dorsal column oligodendrocyte (R^2=0.49) and microvessel (R^2=0.57) loss both correlated well with sensory axon loss (p<0.01 for each; Figure 12C).

To further identify the importance of the length of oligodendrocyte and microvessel loss as contributing to sensory axon loss, an additional group of rats was administered a single injection of EB, rather than two injections spaced 1.5 mm apart. This might determine whether damage to the epicenter, but not penumbra, would spare sensory axons. A single injection of 0.3 μg/μl EB gave similar effects at the epicenter with the number of APC+ cells significantly decreased to 26 ± 4% of sham 7 days after injection (p<0.001), which was not different than those receiving two injections (p>0.05; data not shown). Myelin was also decreased at the epicenter in those receiving a single EB injection (32 ± 13%; p<0.0001, Figure 10B), which was not different than those receiving two injections (23 ± 9%; p>0.05, Figure 10B). Similarly, decreases in the number of LEA+ microvessels at the epicenter were observed in rats receiving only a single injection of EB (p<0.05; Figure 9D), though the extent of loss was not to the degree of two injections at 3 or 7 days (p<0.05 and p<0.01 respectively; Figure 9D). As expected, the greatest difference between single and double EB injections was the length of oligodendrocyte and microvessel loss, which was much less in those receiving single versus double injections (0.9 ± 0.4 vs. 3.8 ± 0.5 mm for APC, p<0.05; 0.2 ± 0.1 vs. 2.5 ± 0.6 mm respectively for LEA, p<0.01; Figure 9C). Therefore, a single EB injection did indeed damage the epicenter but not the penumbra. Importantly, when a single injection of 0.3 μg/μl EB was delivered sensory axons remained intact and the CTB values were not different from sham (p>0.05, Figure 11B) and were significantly higher than those from rats receiving two injections at 7 days (p<0.05; Figure 11B). This further highlights the fact that penumbral loss of oligodendrocytes and microvessels after EB plays a major role in the sensor axon loss observed.

Dorsal column selective EB lesions cause grid walking deficits

Injections of 0.3 μg/μl EB, which caused sensory axon loss (Figure 11B, 42d EB) caused deficits in the grid walking test, where EB treated rats had more footfalls than saline injected rats (p<0.001; Figure 13A). On average EB injected rats made more footfall errors than those injected with saline over the five week period (p<0.001; Figure 13B). Further, within the EB treated animals, the average number of footfalls directly correlated with the degree of sensory axon loss (R^2=0.58; p<0.05; Figure 13C). In contrast, EB did not induce any meaningful deficits on overground locomotion as assessed with the BBB test. A statistically significant effect was observed only at 1 week post injection (p<0.05; Figure 13D) but it was very small, with EB- and saline-treated averaging a score of 20 and 21, respectively, reflecting some trunk instability.

Discussion

Ischemia causes axon loss

Our previous studies showed in a very similar mild contusion injury of the dorsal columns like we used in the present study that intrathecal infusion of a protein tyrosine phosphatase inhibitor could rescue the ascending primary sensory axons as well as the surrounding microvessels and tissue (Nakashima et al., 2008). This suggested that microvascular loss might cause degeneration of axons, which was addressed in this study. This idea is also supported by our finding that rescue of microvessels with endothelial-specific angiopoietin-1 also spares white matter (Han et al 2010). Here, the mild contusive SCI induced acute ischemia in the dorsal columns as shown by the loss of blood flow in microvessels at the epicenter raising the possibility that the sensory axon loss might be caused by endothelial cell loss. This acute loss of perfusion and subsequent endothelial cell loss has been shown after moderate contusions in rats (Muradov and Hagg, 2013), or in monkeys (Fried and Goodkin, 1971) as well in compression in rats (Koyanagi et al., 1993). Here, by 3 hours only 20% of epicenter microvessels remained perfused as identified by intravenously injected LEA, which binds to glucosamines on endothelial cells (Jilani et al., 2003). The degree of microvessel loss progressively worsened, with only 7% of epicenter and 15% penumbra microvessels remaining at 12 hours after injury. This shows that ischemia persists in the injured dorsal white matter and that there is no reperfusion phase in the penumbra which we previously had found when we included analyses of the more vascular gray matter (Muradov and Hagg, 2013).

This difference may be caused by the fact that the dorsal columns are perfused by blood vessels which penetrate from the dorso-lateral side of the spinal cord and are thus more severely injured by the dorsal impact than the ventral blood vessels which mainly serve the gray matter (Martirosyan et al., 2011, Tator and Koyanagi, 1997). This study also confirmed the existence of vasospasm by finding fewer LEA labeled microvessels than those identified by endothelial markers (Benton et al., 2009, Han et al., 2010, Muradov and Hagg, 2013, Myers et al., 2011). The adjacent penumbra (1 mm rostral and caudal to the epicenter) followed a similar progression, but with less extensive damage as the epicenter. This ‘wave’ of damage may be caused by death of endothelial cells (Stempien-Otero et al., 1999), breakdown of neurovascular control (Rivlin and Tator, 1978), release of vasoactive substances (Osterholm and Mathews, 1972) and possibly by leakage of serum proteins (Sharma, 2003, Whetstone et al., 2003). In EAE models the serum protein fibrinogen can contribute to axonal damage (Davalos et al., 2012). Whether serum proteins directly or indirectly contribute to axonal damage acutely after spinal cord injury remains to be determined.

The ascending primary sensory axons of the dorsal column degenerate starting sometime after 4 hours post-injury because we can rescue them all by a treatment which starts after 4 hours using a similar dorsal column injury severity in rats (Nakashima et al., 2008). Here, these axons had degenerated within 24 hours after the contusive injury, which is the earliest time point we were able to document axon sparing by anterograde tracing. We did not use other types of analyses to try to define the time course more precisely. Analyses of degenerating axons at the injury site by histological means do not provide conclusive data about axonal interruption and we did not perform those. For example, neurofilament and APP have been used to show changes in axons at the epicenter (Li et al., 1995), but the contusion produces a long region of axonal injury and swelling, which makes it impossible to identify axons that actually have been severed. Contusive or compressive SCI disrupts axonal conduction within minutes even though viable axons are still present (James et al., 2011). Our own unpublished data show that conduction of sensory evoked potentials from the sciatic nerve to the nucleus gracilis is lost starting after 20 minutes and is complete by 3

hours. This limits the use of electrophysiological measures in determining acutely when axon loss occurs after SCI. Because of this we assessed axon loss after SCI by tracing dorsal column sensory axons with CTB (Baker et al., 2007). One disadvantage of using the CTB tracing method is the relatively long time after sciatic injection (~48 hours) it takes for the tracer to fill all the terminals in the nucleus gracilis. For this reason sciatic injection of CTB was done 24 hours before SCI, which resulted in only minimal tracing to the medulla at 24 hours, thus permitting assessment of sensory axons after another 24 hours, e.g., post-injury. We did not use longer pre-injury protocols because all axonal projections would be labeled, making it impossible to define the extent of axons loss that occurred at the epicenter at any given time early post-injury. Our data suggest that 30% of sensory axons can be detected at 24 hours after a 120 kdyn contusive SCI. Approximately 14% of these projections would be labeled by our current pre-injection method at the time of the injury suggesting that as few as ~16% of axons in the current study remained intact after SCI. Either way, we conclude that overwhelmingly most of the axon loss after SCI occurs between 4 and 24 hours.

It remains, therefore, unclear whether persistent ischemia and loss of microvessels beyond the 4 hours following the contusive injury coincides with the observed axon loss. To address the question whether the ischemia might cause axon loss we utilized a phototoxic ischemia model (Bunge et al., 1994). This model results in local thrombosis due to attachment of rose bengal molecules to platelets during illumination with green light. Further, this model also results in some reperfusion, extensive inflammatory changes and loss of gray and white matter around the ischemic injury site (Bunge et al., 1994, Itoh et al., 2010, Paíno et al., 1994, von Euler et al., 1997). As such, it mimics several key aspects of contusive injury. Importantly, this model specifically targets blood vessels and the observed effects on axons can be attributed to ischemia. The rapid focal ischemia of the spinal cord after phototoxic injury closely resembles microvascular pathology after SCI. By 24 hours only 8% of microvessels remained in the dorsal columns at the injury epicenter and 45% at the adjacent penumbra, which is largely comparable to 7% and 17%, respectively, seen 12 hours after the contusion. The 24-hour time point was chosen since it corresponds to the earliest time we can measure axon survival using the CTB tracing method. The phototoxic ischemia led to a loss of approximately half of the sensory axons 24 hours post-injury. Phototoxic injury has been shown to demyelinate sub-pial dorsal column axons by 48 hours, with suggestions of regeneration small diameter axons occurring (Olby and Blakemore, 1996). Our injury seems to be more severe thus perhaps resulting in acute axonal degeneration. In optic nerve slices, ischemia causes inhibition of axonal function within minutes related to failure of Na^+-K^+-ATPase with accumulation of Na^+ inside the cell (Stys, 2004). This in turn activates Na^+-Ca^{++} exchange and leads to axonal Ca^{++} overload (Stys, 1998). Thus, pure ischemic injury can cause axonal loss. The axonal degeneration seen after the contusive injury may not only be due to ischemia because of the greater numbers of surviving axons seen in the phototoxic injury. The percentage of CTB+ projections was decreased to 53 ± 6% of sham (Figure 6, $p<0.05$), which is significantly higher when compared to the contusion injury (30 ± 4%, $p<0.01$). The greater sensory axon loss (~23%) after contusive SCI may reflect the degenerative effects of other factors, including mechanical impact and/or other secondary events other than ischemia. On the other hand, because of the greater number of microvessels observed at the penumbra after the phototoxic injury it is possible that it was not severe enough to mimic the contusive injury.

The penumbra is important for axonal survival

Importantly, our results reveal a direct correlation between length of microvascular hypoperfusion and axonal loss, i.e., ischemic injury along the axis of the spinal cord and the degree of axon degeneration. These findings suggest that if the ischemia is confined over short distances along the axons they do not degenerate. More than 50% of the axons can

survive without vessels at the epicenter, suggesting that a sufficient axial length of penumbra is important for axonal survival. Similar to phototoxic ischemia, the length of microvessel damage following EB injections correlated with axon loss. Most evidently, there was no axon loss after single injections of EB which resulted in a similar loss of microvessels at the epicenter as seen with EB injections into two sites separated by 1.5 mm, but without the loss of penumbral microvessels. This further confirms that the penumbral spread of ischemia is key to axon loss. There seems to be an ~2 mm threshold before fatal axonal damage occurs. We propose that this is most likely also true for other nervous system injuries, which involve temporary or permanent ischemia, including SCI, traumatic brain injury, and stroke.

The extent of white matter sparing at the thoracic injury epicenter is predictive of hindlimb locomotor function in rodents (Basso et al., 1996, Han et al., 2010, Li et al., 2006). This study suggests the importance of the penumbral tissue preservation for the maintenance of axons traveling through the injury. For example, the extent of axon preservation correlated not with the epicenter preservation but with the injury length. Thus, it is not just the epicenter, but the length of injury that is important, as shown in both the phototoxic and EB models. After a contusive injury, there is a progressive loss over 12 hr of cells in the penumbra. This may explain why we could wait 4 hours after injury and still maintain all the sensory axons after a similar injury severity (Nakashima et al., 2008). If so, this might provide an opportunity to improve therapies by targeting the pathophysiological mechanisms in the penumbra. One such mechanisms might be hypoperfusion due to vasospasm which intravenous infusions of magnesium can resolve better in the penumbra than in the epicenter (Muradov and Hagg, 2013).

Potential role of oligodendrocyte loss in axon loss

Oligodendrocytes are thought to contribute to the support of axonal integrity through maintenance of the myelin sheath as well as by providing neurotrophic and metabolic support (Nave and Trapp, 2008, Rinholm et al., 2011). Similar to length of ischemia, loss of sensory axons after phototoxic injury is highly correlated to length of oligodendrocyte loss. Therefore, we explored whether the axonal degeneration after SCI or pure ischemia was due to acute loss of oligodendrocytes. To test this, the glial toxin EB was administered in an attempt selectively ablate oligodendrocytes in the dorsal column. EB is a DNA intercalator which is known to kill glial cells around the injection site (Blakemore, 1982). EB (0.3 μg/μl) permanently eliminated most of the dorsal column oligodendrocytes as assessed as early as three days after injection and led to a 56% loss of dorsal column sensory axons. However, EB injections also resulted in an unexpected localized hypoperfusion, similar in magnitude to contusive SCI and phototoxic ischemia. The loss of microvasculature, oligodendrocytes and axons was highly correlated, which would be consistent with degeneration of oligodendrocytes mediating axon loss. However, axons were lost only in rats that received 0.3 μg/μl EB, where perfused vascular loss was seen only at that dose, whereas many oligodendrocytes were lost with 0.1 μg/μl (more than 50% over a 2 mm stretch), yet not resulting in axon loss. The length of oligodendrocyte and vascular damage correlated with axon loss but that was due to the animals with 0.3 μg/μl EB. These data suggest that ischemia is the main cause of axon loss following SCI but that acute oligodendrocyte loss might contribute as long as it is over a substantial axial distance.

One main mechanism by which ischemia might cause axon loss is the loss of metabolic support from blood vessels to axons, which is necessary for their maintenance, and is mediated by oligodendrocytes (Nave and Trapp, 2008, Rinholm et al., 2011). For instance, blood-derived glucose is converted to lactate in oligodendrocytes and is shuttled to axons via the monocarboxylate transporter 1 (MCT1). Disruption of spinal MCT1 induces motor neuron loss (Lee et al., 2012). Therefore, the ischemia-induced dysfunction and loss of

oligodendrocytes might lead to a reduced presence of mitochondrial energy substrate in the sensory axons. Such loss of ATP would lead to failure of Na^+-K^+-ATPase with accumulation of Na^+ inside the cell (Stys, 2004) and activation of Na^+-Ca^{++} exchange resulting in axonal Ca^{++} overload (Stys, 1998). However, these potential mechanisms remain to be defined within the dorsal column injury models.

Sensory axon degeneration in the SCI and EB experimental models mostly occurred before the development of demyelination. Therefore, loss of myelin is not indicated as the primary cause of axon degeneration in these models. It was shown similarly (Smith et al., 2013). In a separate set of experiments following a mild contusion we have shown that temporary protection of myelin with intrathecal minocycline infusion for 7 days does not lead to improved axon sparing (Nakashima and Hagg, unpublished). Collectively, these findings suggest that demyelination is not the primary cause of acute axon loss following SCI.

Interestingly, the degree of epicenter hypoperfusion and loss of oligodendrocytes across all concentrations of EB assessed was highly correlated (r^2=0.81). Even in these lower dose groups (0.01 – 0.1 μg/μl) numbers of remaining dorsal column oligodendrocytes and blood vessels remained highly correlated (R^2=0.70, $p<0.01$). This indicates that oligodendrocyte loss from EB might be mediated through vascular disruption. Oligodendrocytes are sensitive to disruption of oxygen and glucose (Lee et al., 2012, Rinholm et al., 2011). Indeed, the phototoxic ischemia caused a substantial loss of oligodendrocytes at the epicenter and penumbra. This was seen as far away as 2 mm from the epicenter at 24 hours, even though perfused blood vessels remained present. This suggests that penumbral oligodendrocytes are more susceptible than endothelial cells after temporary ischemia.

The grid walk test assesses dorsal column function

Dorsal column sensory axon degeneration after EB injection resulted in functional deficits over a 42-day period. Whereas overground locomotion as assessed by the BBB scale was barely if at all affected the grid walking test showed meaningful differences, with EB rats having twice as many footfalls as saline injected ones. This is consistent with previous work showing that EB injections in the dorsal column results in decreased performance on a ladder (Blakemore, 1982). Dorsal column transection also induces impairments on ladder (Webb and Muir, 2003) and grid walking (Schucht et al., 2002). Moreover, in our own experiments using the exact same grid walk device and parameters, rescue of the ascending sensory axons after a contusive injury correlated highly with the grid walking performance (Nakashima et al., 2008). This provides further support of using grid walking or ladder performance to assess dorsal column axon integrity.

Conclusion

In conclusion, the current study indicates that ischemia and endothelial cell loss leads to oligodendrocyte and axon degeneration after SCI. It is possible that ischemia-induced loss of oligodendrocytes causes failure of their metabolic support for axons, leading to loss of axonal ATP thus increasing pathological Na^+ and Ca^{++} levels and axonal disruption. We suggest that treating ongoing ischemia after SCI is an important and necessary target for successful preserving long projecting axons and locomotor function. Most importantly, the current work illustrates that ischemia beyond approximately a 1–2 mm stretch along the length of an axon results in degeneration. This suggests that protection of the penumbral vessels against secondary degeneration is essential.

Acknowledgments

We wish to thank Yun Shi Long, Hillary Conway, Sheila Arnold, Christine Yarberry, Kim Cash and Darlene Burke for their excellent technical assistance. This work was supported by a grant from the Kentucky Spinal Cord and

Head Injury Trust, and by NIH grants NS045734 and GM103507, Norton Healthcare, and the Commonwealth of Kentucky Challenge for Excellence.

References

Alford PW, Dabiri BE, Goss JA, Hemphill MA, Brigham MD, Parker KK. Blast-induced phenotypic switching in cerebral vasospasm. Proceedings of the National Academy of Sciences of the United States of America. 2011; 108:12705–12710. [PubMed: 21765001]

Almad A, Sahinkaya FR, McTigue DM. Oligodendrocyte fate after spinal cord injury. Neurotherapeutics. 2011; 8:262–273. [PubMed: 21404073]

Anthes DL, Theriault E, Tator CH. Characterization of axonal ultrastructural pathology following experimental spinal cord compression injury. Brain research. 1995; 702:1–16. [PubMed: 8846063]

Baker KA, Hagg T. An adult rat spinal cord contusion model of sensory axon degeneration: the estrus cycle or a preconditioning lesion do not affect outcome. Journal of neurotrauma. 2005; 22:415–428. [PubMed: 15853460]

Baker KA, Nakashima S, Hagg T. Dorsal column sensory axons lack TrkC and are not rescued by local neurotrophin-3 infusions following spinal cord contusion in adult rats. Experimental neurology. 2007; 205:82–91. [PubMed: 17316612]

Basso DM, Beattie MS, Bresnahan JC. Graded histological and locomotor outcomes after spinal cord contusion using the NYU weight-drop device versus transection. Experimental neurology. 1996; 139:244–256. [PubMed: 8654527]

Benton RL, Hagg T. Vascular Pathology as a Potential Therapeutic Target in SCI. Translational Stroke Research. 2011; 2:556–574.

Benton RL, Maddie MA, Dincman TA, Hagg T, Whittemore SR. Transcriptional activation of endothelial cells by TGFβ coincides with acute microvascular plasticity following focal spinal cord ischaemia/reperfusion injury. ASN neuro. 2009; 1:e00015. [PubMed: 19663807]

Benton RL, Maddie MA, Minnillo DR, Hagg T, Whittemore SR. Griffonia simplicifolia isolectin B4 identifies a specific subpopulation of angiogenic blood vessels following contusive spinal cord injury in the adult mouse. The Journal of comparative neurology. 2008; 507:1031–1052. [PubMed: 18092342]

Blakemore WF. Ethidium bromide induced demyelination in the spinal cord of the cat. Neuropathology and applied neurobiology. 1982; 8:365–375. [PubMed: 7177337]

Bunge MB, Holets VR, Bates ML, Clarke TS, Watson BD. Characterization of photochemically induced spinal cord injury in the rat by light and electron microscopy. Experimental neurology. 1994; 127:76–93. [PubMed: 8200439]

Cao Q, Zhang YP, Iannotti C, DeVries WH, Xu X-M, Shields CB, Whittemore SR. Functional and electrophysiological changes after graded traumatic spinal cord injury in adult rat. Experimental neurology. 2005; 191:S3–S16. [PubMed: 15629760]

Davalos D, Ryu JK, Merlini M, Baeten KM, Le Moan N, Petersen MA, Deerinck TJ, Smirnoff DS, Bedard C, Hakozaki H, Gonias Murray S, Ling JB, Lassmann H, Degen JL, Ellisman MH, Akassoglou K. Fibrinogen-induced perivascular microglial clustering is required for the development of axonal damage in neuroinflammation. Nature communications. 2012; 3:1227.

Donnelly DJ, Popovich PG. Inflammation and its role in neuroprotection, axonal regeneration and functional recovery after spinal cord injury. Experimental neurology. 2008; 209:378–388. [PubMed: 17662717]

Ek CJ, Habgood MD, Callaway JK, Dennis R, Dziegielewska KM, Johansson PA, Potter A, Wheaton B, Saunders NR. Spatio-temporal progression of grey and white matter damage following contusion injury in rat spinal cord. PloS one. 2010; 5:e12021. [PubMed: 20711496]

Fassbender JM, Whittemore SR, Hagg T. Targeting microvasculature for neuroprotection after SCI. Neurotherapeutics. 2011; 8:240–251. [PubMed: 21360237]

Fehlings MG, Tator CH. The relationships among the severity of spinal cord injury, residual neurological function, axon counts, and counts of retrogradely labeled neurons after experimental spinal cord injury. Experimental neurology. 1995; 132:220–228. [PubMed: 7789460]

Frei E, Klusman I, Schnell L, Schwab ME. Reactions of oligodendrocytes to spinal cord injury: cell survival and myelin repair. Experimental neurology. 2000; 163:373–380. [PubMed: 10833310]

Fried LC, Goodkin R. Microangiographic observations of the experimentally traumatized spinal cord. Journal of neurosurgery. 1971; 35:709–714. [PubMed: 5000663]

Fünfschilling U, Supplie LM, Mahad D, Boretius S, Saab AS, Edgar J, Brinkmann BG, Kassmann CM, Tzvetanova ID, Möbius W, Diaz F, Meijer D, Suter U, Hamprecht B, Sereda MW, Moraes CT, Frahm J, Goebbels S, Nave K-A. Glycolytic oligodendrocytes maintain myelin and long-term axonal integrity. Nature. 2012; 485:517–521. [PubMed: 22622581]

Guha A, Tator CH, Smith CR, Piper I. Improvement in post-traumatic spinal cord blood flow with a combination of a calcium channel blocker and a vasopressor. The Journal of trauma. 1989; 29:1440–1447. [PubMed: 2810423]

Han S, Arnold SA, Sithu SD, Mahoney ET, Geralds JT, Tran P, Benton RL, Maddie MA, D'Souza SE, Whittemore SR, Hagg T. Rescuing vasculature with intravenous angiopoietin-1 and alpha v beta 3 integrin peptide is protective after spinal cord injury. Brain. 2010; 133:1026–1042. [PubMed: 20375135]

Itoh Y, Toriumi H, Yamada S, Hoshino H, Suzuki N. Resident endothelial cells surrounding damaged arterial endothelium reendothelialize the lesion. Arteriosclerosis, thrombosis, and vascular biology. 2010; 30:1725–1732.

James ND, Bartus K, Grist J, Bennett DLH, McMahon SB, Bradbury EJ. Conduction failure following spinal cord injury: functional and anatomical changes from acute to chronic stages. The Journal of neuroscience. 2011; 31:18543–18555. [PubMed: 22171053]

Jilani SM, Murphy TJ, Thai SNM, Eichmann A, Alva JA, Iruela-Arispe ML. Selective binding of lectins to embryonic chicken vasculature. The journal of histochemistry and cytochemistry. 2003; 51:597–604. [PubMed: 12704207]

Koyanagi I, Tator CH, Theriault E. Silicone rubber microangiography of acute spinal cord injury in the rat. Neurosurgery. 1993; 32:260–268. [PubMed: 8437664]

Lee Y, Morrison BM, Li Y, Lengacher S, Farah MH, Hoffman PN, Liu Y, Tsingalia A, Jin L, Zhang P-W, Pellerin L, Magistretti PJ, Rothstein JD. Oligodendroglia metabolically support axons and contribute to neurodegeneration. Nature. 2012; 487:443–448. [PubMed: 22801498]

Li GL, Farooque M, Holtz A, Olsson Y. Changes of beta-amyloid precursor protein after compression trauma to the spinal cord: an experimental study in the rat using immunohistochemistry. Journal of neurotrauma. 1995; 12:269–277. [PubMed: 7473801]

Li Y, Oskouian RJ, Day Y-J, Kern JA, Linden J. Optimization of a mouse locomotor rating system to evaluate compression-induced spinal cord injury: correlation of locomotor and morphological injury indices. Journal of neurosurgery. Spine. 2006; 4:165–173. [PubMed: 16506485]

Maikos JT, Qian Z, Metaxas D, Shreiber DI. Finite element analysis of spinal cord injury in the rat. Journal of neurotrauma. 2008; 25:795–816. [PubMed: 18627257]

Martirosyan NL, Feuerstein JS, Theodore N, Cavalcanti DD, Spetzler RF, Preul MC. Blood supply and vascular reactivity of the spinal cord under normal and pathological conditions. Journal of neurosurgery. Spine. 2011; 15:238–251. [PubMed: 21663407]

Mautes AE, Bergeron M, Sharp FR, Panter SS, Weinzierl M, Guenther K, Noble LJ. Sustained induction of heme oxygenase-1 in the traumatized spinal cord. Experimental neurology. 2000; 166:254–265. [PubMed: 11085891]

Misgeld T, Nikic I, Kerschensteiner M. In vivo imaging of single axons in the mouse spinal cord. Nature protocols. 2007; 2:263–268.

Muradov JM, Hagg T. Intravenous Infusion of Magnesium Chloride Improves Epicenter Blood Flow during the Acute Stage of Contusive Spinal Cord Injury in Rats. Journal of neurotrauma. 2013; 30:840–852. [PubMed: 23302047]

Myers SA, DeVries WH, Andres KR, Gruenthal MJ, Benton RL, Hoying JB, Hagg T, Whittemore SR. CD47 knockout mice exhibit improved recovery from spinal cord injury. Neurobiology of disease. 2011; 42:21–34. [PubMed: 21168495]

Nakashima S, Arnold SA, Mahoney ET, Sithu SD, Zhang YP, D'Souza SE, Shields CB, Hagg T. Small-molecule protein tyrosine phosphatase inhibition as a neuroprotective treatment after

spinal cord injury in adult rats. The Journal of neuroscience. 2008; 28:7293–7303. [PubMed: 18632933]

Nave K-A, Trapp BD. Axon-glial signaling and the glial support of axon function. Annual review of neuroscience. 2008; 31:535–561.

Olby NJ, Blakemore WF. Primary demyelination and regeneration of ascending axons in the dorsal funiculus of the rat spinal cord following photochemically induced injury. Journal of neurocytology. 1996; 25:465–480. [PubMed: 8899568]

Osterholm JL, Mathews GJ. Altered norepinephrine metabolism following experimental spinal cord injury. 1. Relationship to hemorrhagic necrosis and post-wounding neurological deficits. Journal of neurosurgery. 1972; 36:386–394. [PubMed: 5013609]

Paíno CL, Fernandez-Valle C, Bates ML, Bunge MB. Regrowth of axons in lesioned adult rat spinal cord: promotion by implants of cultured Schwann cells. Journal of neurocytology. 1994; 23:433–452. [PubMed: 7964912]

Rabchevsky AG, Fugaccia I, Sullivan PG, Scheff SW. Cyclosporin A treatment following spinal cord injury to the rat: behavioral effects and stereological assessment of tissue sparing. Journal of neurotrauma. 2001; 18:513–522. [PubMed: 11393254]

Rinholm JE, Hamilton NB, Kessaris N, Richardson WD, Bergersen LH, Attwell D. Regulation of oligodendrocyte development and myelination by glucose and lactate. The Journal of neuroscience. 2011; 31:538–548. [PubMed: 21228163]

Rivlin AS, Tator CH. Regional spinal cord blood flow in rats after severe cord trauma. Journal of neurosurgery. 1978; 49:844–853. [PubMed: 731301]

Rosenberg LJ, Zai LJ, Wrathall JR. Chronic alterations in the cellular composition of spinal cord white matter following contusion injury. Glia. 2005; 49:107–120. [PubMed: 15390101]

Schucht P, Raineteau O, Schwab ME, Fouad K. Anatomical correlates of locomotor recovery following dorsal and ventral lesions of the rat spinal cord. Experimental neurology. 2002; 176:143–153. [PubMed: 12093091]

Sharma HS. Neurotrophic factors attenuate microvascular permeability disturbances and axonal injury following trauma to the rat spinal cord. Acta neurochirurgica. Supplement. 2003; 86:383–388. [PubMed: 14753473]

Shields LBE, Zhang YP, Burke DA, Gray R, Shields CB. Benefit of chondroitinase ABC on sensory axon regeneration in a laceration model of spinal cord injury in the rat. Surgical neurology. 2008; 69:568–577. [PubMed: 18486695]

Smith CM, Cooksey E, Duncan ID. Myelin loss does not lead to axonal degeneration in a long-lived model of chronic demyelination. The Journal of neuroscience : the official journal of the Society for Neuroscience. 2013; 33:2718–2727. [PubMed: 23392698]

Stempien-Otero A, Karsan A, Cornejo CJ, Xiang H, Eunson T, Morrison RS, Kay M, Winn R, Harlan J. Mechanisms of hypoxia-induced endothelial cell death. Role of p53 in apoptosis. The Journal of biological chemistry. 1999; 274:8039–8045. [PubMed: 10075703]

Stys PK. Anoxic and ischemic injury of myelinated axons in CNS white matter: from mechanistic concepts to therapeutics. Journal of cerebral blood flow and metabolism. 1998; 18:2–25. [PubMed: 9428302]

Stys PK. White matter injury mechanisms. Current molecular medicine. 2004; 4:113–130. [PubMed: 15032708]

Tator CH, Koyanagi I. Vascular mechanisms in the pathophysiology of human spinal cord injury. Journal of neurosurgery. 1997; 86:483–492. [PubMed: 9046306]

von Euler M, Sundström E, Seiger A. Morphological characterization of the evolving rat spinal cord injury after photochemically induced ischemia. Acta neuropathologica. 1997; 94:232–239. [PubMed: 9292692]

Webb AA, Muir GD. Unilateral dorsal column and rubrospinal tract injuries affect overground locomotion in the unrestrained rat. The European journal of neuroscience. 2003; 18:412–422. [PubMed: 12887423]

Whetstone WD, Hsu JY, Eisenberg M, Werb Z, Noble-Haeusslein LJ. Blood-spinal cord barrier after spinal cord injury: relation to revascularization and wound healing. Journal of neuroscience research. 2003; 74:227–239. [PubMed: 14515352]

Highlights

- Contusion causes rapid loss of dorsal column microvessels, oligodendrocytes and axons
- This is caused by microvessel loss as shown by focal ischemia of the dorsal columns
- Penumbral microvessel loss determines axon loss, offering treatment opportunities
- The glial toxin ethidium bromide causes ischemic injury and axonal loss

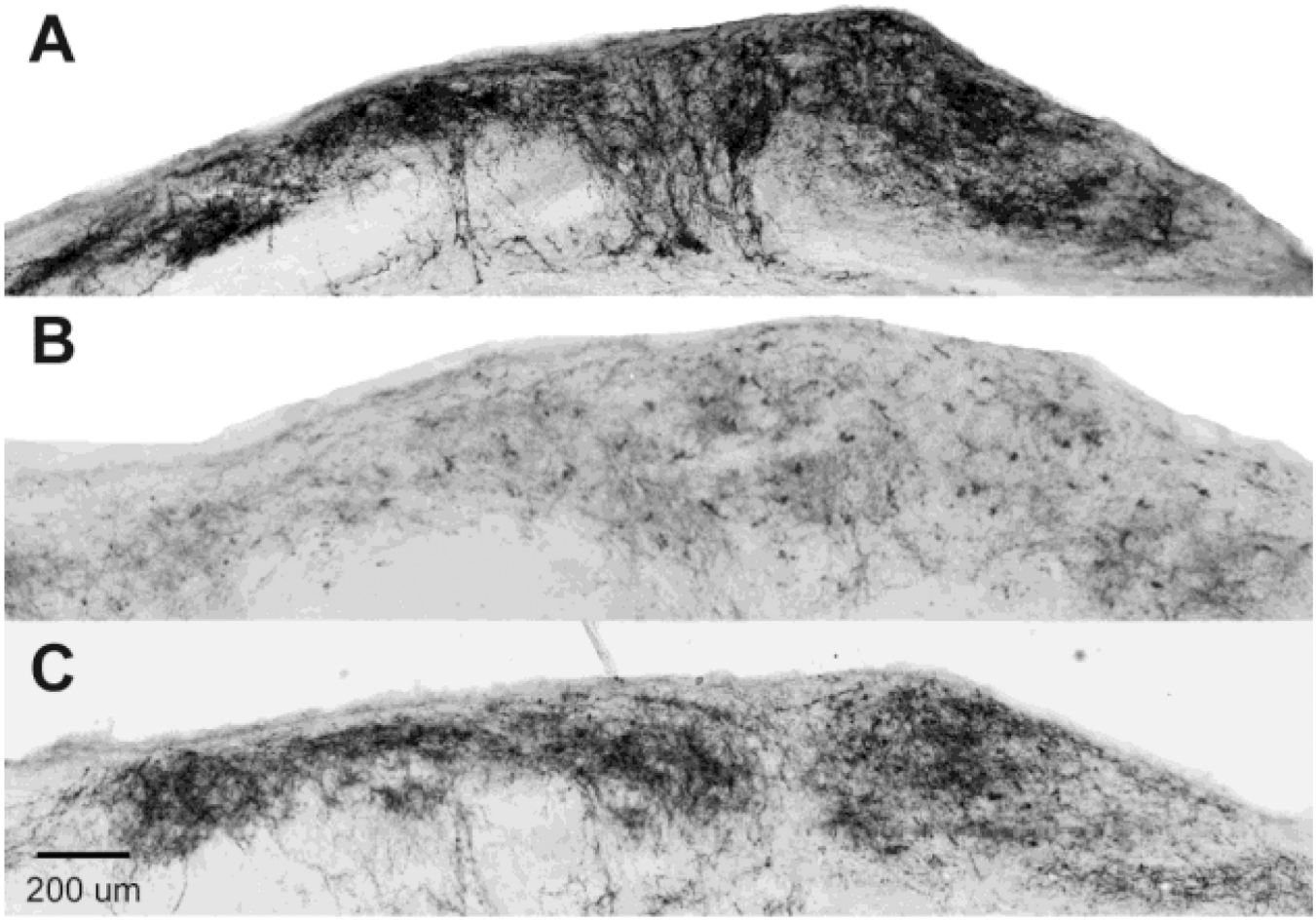

Figure 1. Ascending dorsal column sensory axons are lost 24 hours after a mild contusion

CTB was injected bilaterally into the sciatic nerves 24 hours before injury and CTB labeled axonal projections in the nucleus gracilis of the medulla assessed 24 hours after injury. Compared to Sham rats traced for 48 hours (**A**) very few projections are seen in rats 24 hr after a dorsal column transection (**B**) showing that a 24 hr pre-injury tracing does not label many axons and that most tracing is achieved over the next 24 hr. Rats with a 120 kdyn T9 contusion had fewer CTB-labeled projections (**C**) than sham animals, suggesting that most of their axons degenerate within 24 hours post-injury. Scale bar 200 μm.

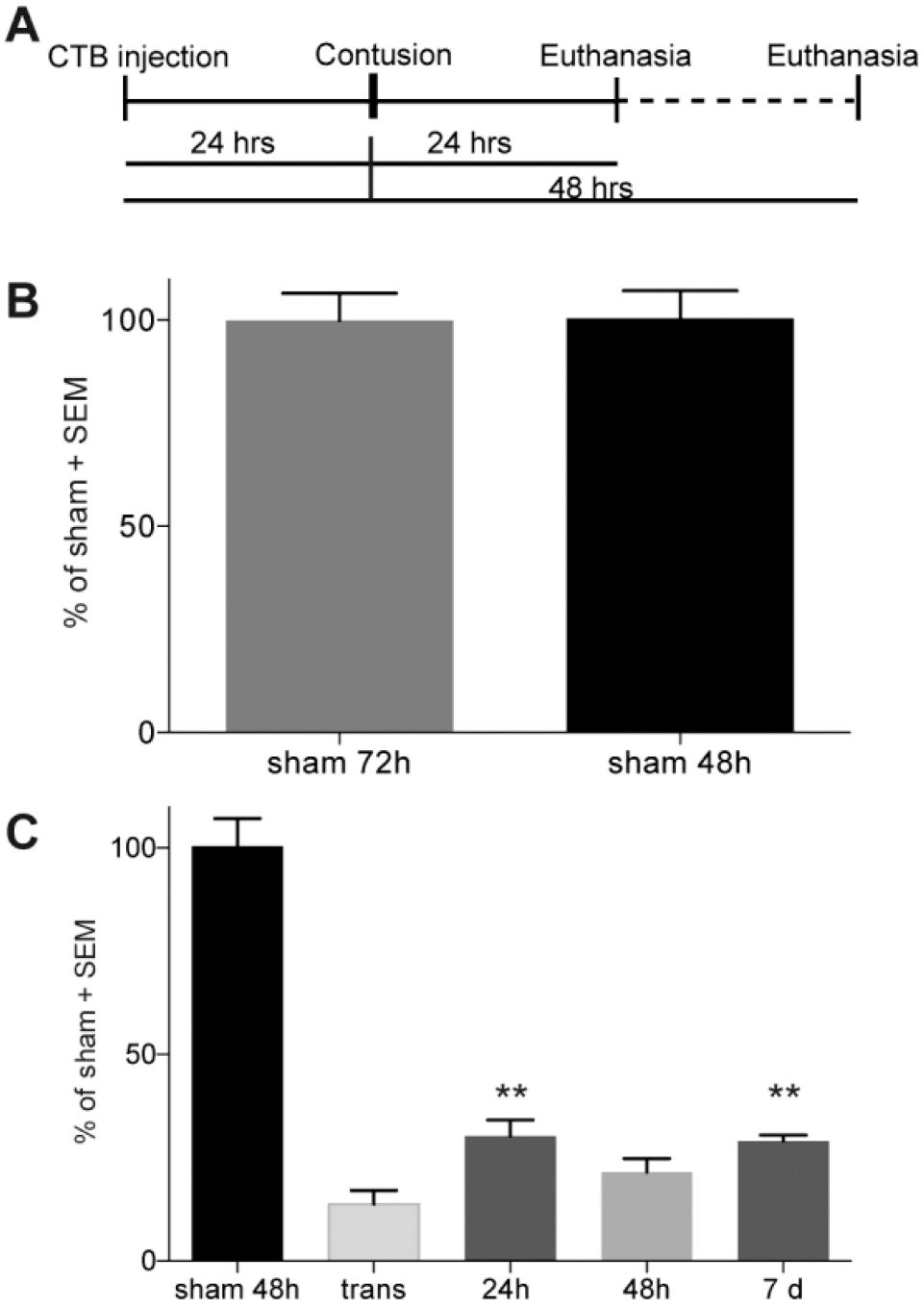

Figure 2. Quantification of dorsal column axon loss after SCI

(**A**) Schematic illustrating the protocol used to determine when sensory axon loss occurs after SCI. CTB was injected bilaterally into the sciatic nerves 24 hours before spinal cord injury at T9 and CTB accumulation in the nucleus gracilis assessed 48 hours later. (**B**) Nucleus gracilis CTB accumulation is similar when assessed either 48 or 72 hours after sciatic nerve injection in sham rats (n=7 for 48 hours; n=9 for 72 hours). (**C**) Few CTB+ projections are seen in the nucleus gracilis of animals with a transection, indicating that most tracing is completed over the next 24 hours. After contusion, fewer axons are seen at 24 hours (n=5), 48 hr (n = 4), and 7 days (n=6) compared to sham, showing that extensive

axonal degeneration occurs within 24 hours. There were more axonal projections after a contusion than with a transection (n=5). **p<0.01 compared to transection using one way ANOVA with Tukey's multiple comparison test.

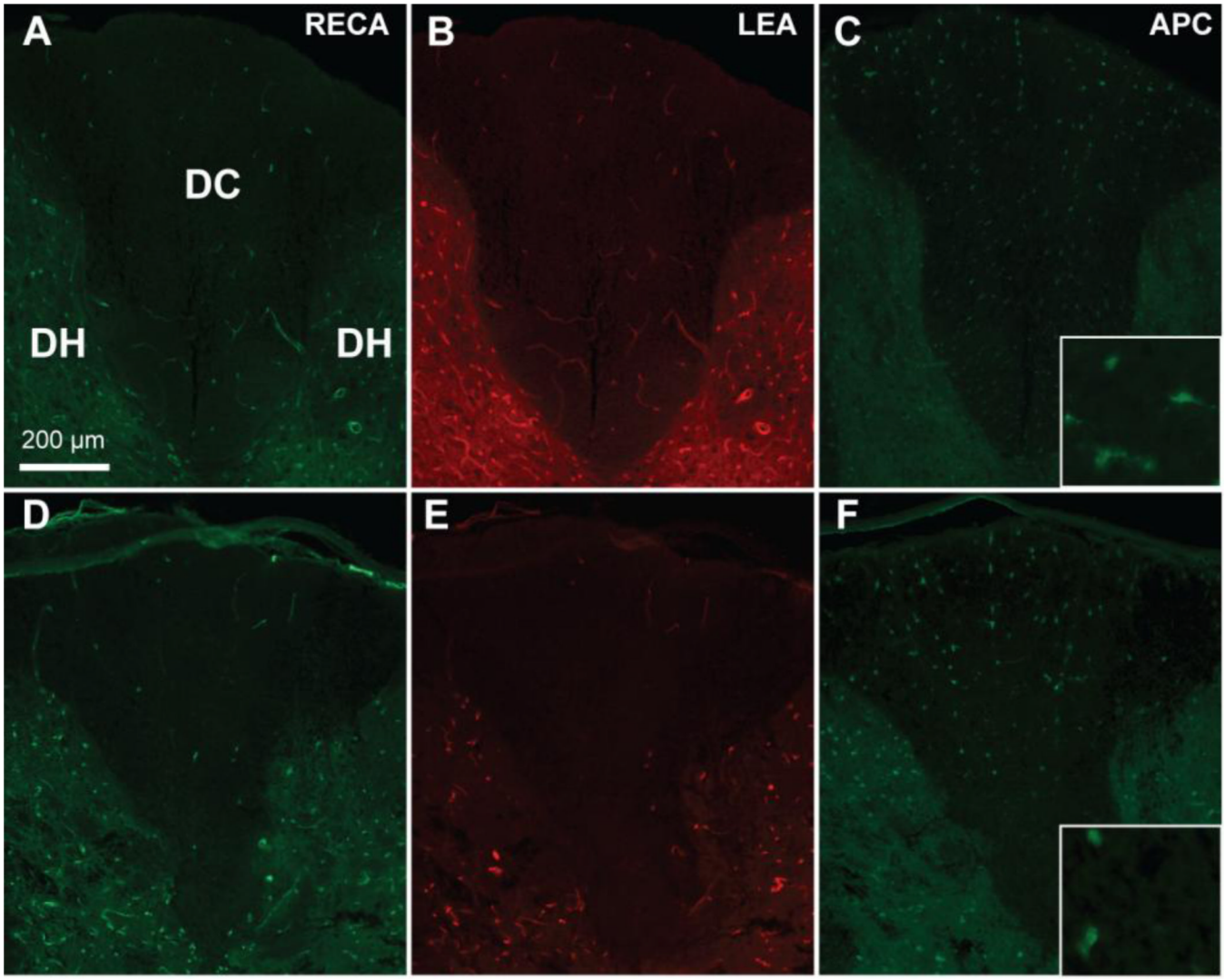

Figure 3. Contusive SCI leads to acute microvascular and oligodendrocyte loss

A 120 kdyn contusion at T9 leads to loss of total (RECA, **D**) and perfused (LEA, **E**) microvessels in the dorsal column compared to sham (**A,B**). Shown here are sections at 1mm rostral to the epicenter from representative rats at 6 hr post-injury. Similarly, APC+ oligodendrocyte loss is observed after contusion (**F**) compared to sham (**C**) in adjacent sections. Insets are 63× objective images APC+ cell bodies. Scale bar 200 μm.

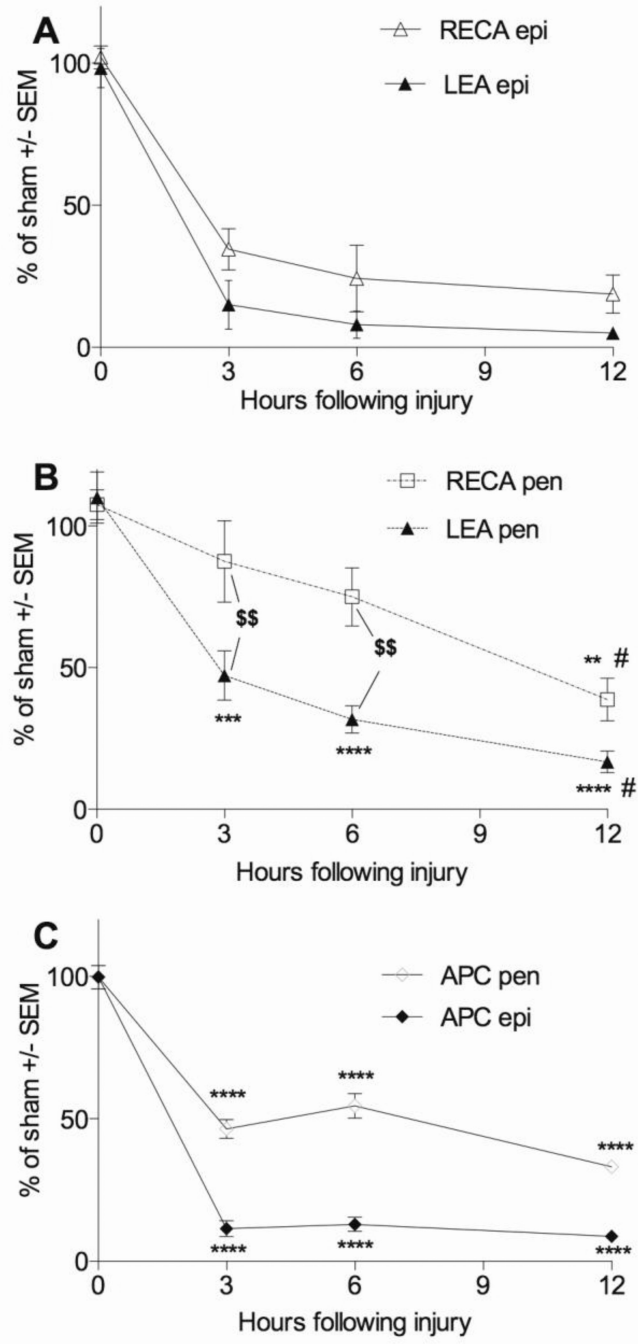

Figure 4. Microvessel and oligodendrocyte loss occurs rapidly after contusive SCI

Microvascular loss is profound by 3 hours after contusion and remains low up to 12 hours at the epicenter **(A)**. Compared to the epicenter, loss of total (RECA) and perfused (LEA) microvessels in the penumbra is more gradual, with more loss observed at 12 hours compared to 3 hours **(B)**. Oligodendrocytes are lost in the epicenter and penumbra occurs by 3 hours and the numbers remain decreased up to 12 hours **(C)** **p<0.01, ***p<0.001, ****p<0.0001 compared to sham; # p<0.05 compared to 3 hours; $$ p<0.01 LEA compared to RECA with two-way ANOVA with Tukey's multiple comparisons' test.

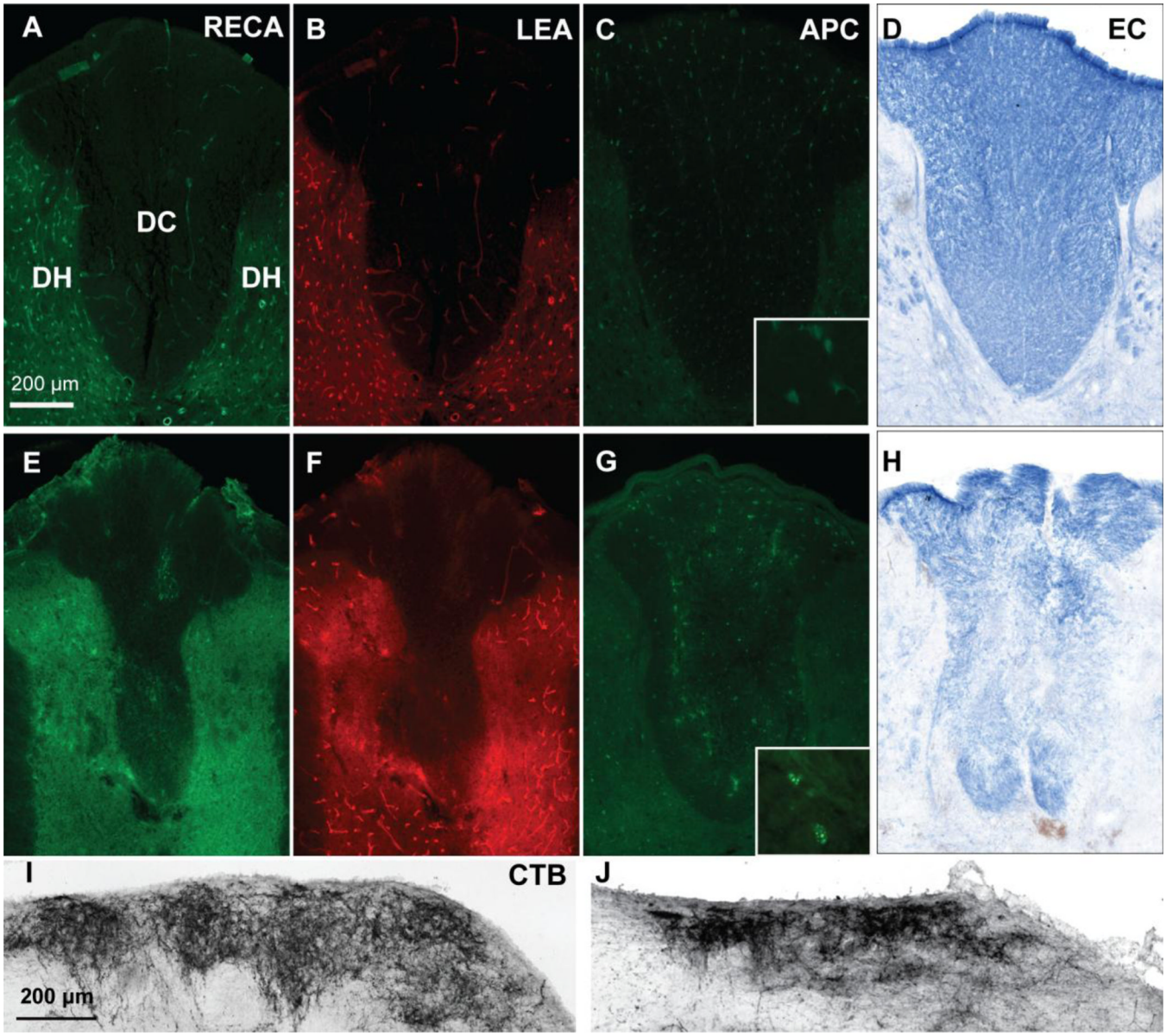

Figure 5. Microvessel, oligodendrocyte, myelin, and sensory axons are lost 24 hours after phototoxic ischemia

Focal phototoxic ischemia of the dorsal column at T9 leads to an almost complete loss of total (RECA, **E**) and perfused (LEA, **F**) dorsal column microvessels compared to sham (**A, B**). Ischemia was also accompanied by severe loss of dorsal column APC+ oligodendrocytes (**G**) compared to sham (**C**), as well as demyelination (**H**, compared to sham, **D**) as assessed with eriochrome cyanine (EC) staining. Dorsal column sensory axon loss was also observed 24 hours after the phototoxic ischemia, as shown by a loss of CTB+ projections in the nucleus gracilis (**J**) compared to sham rats (**I**). Insets (**C, G**) of APC+ cell bodies were taken with a 63× objective. Scale bar 200 μm.

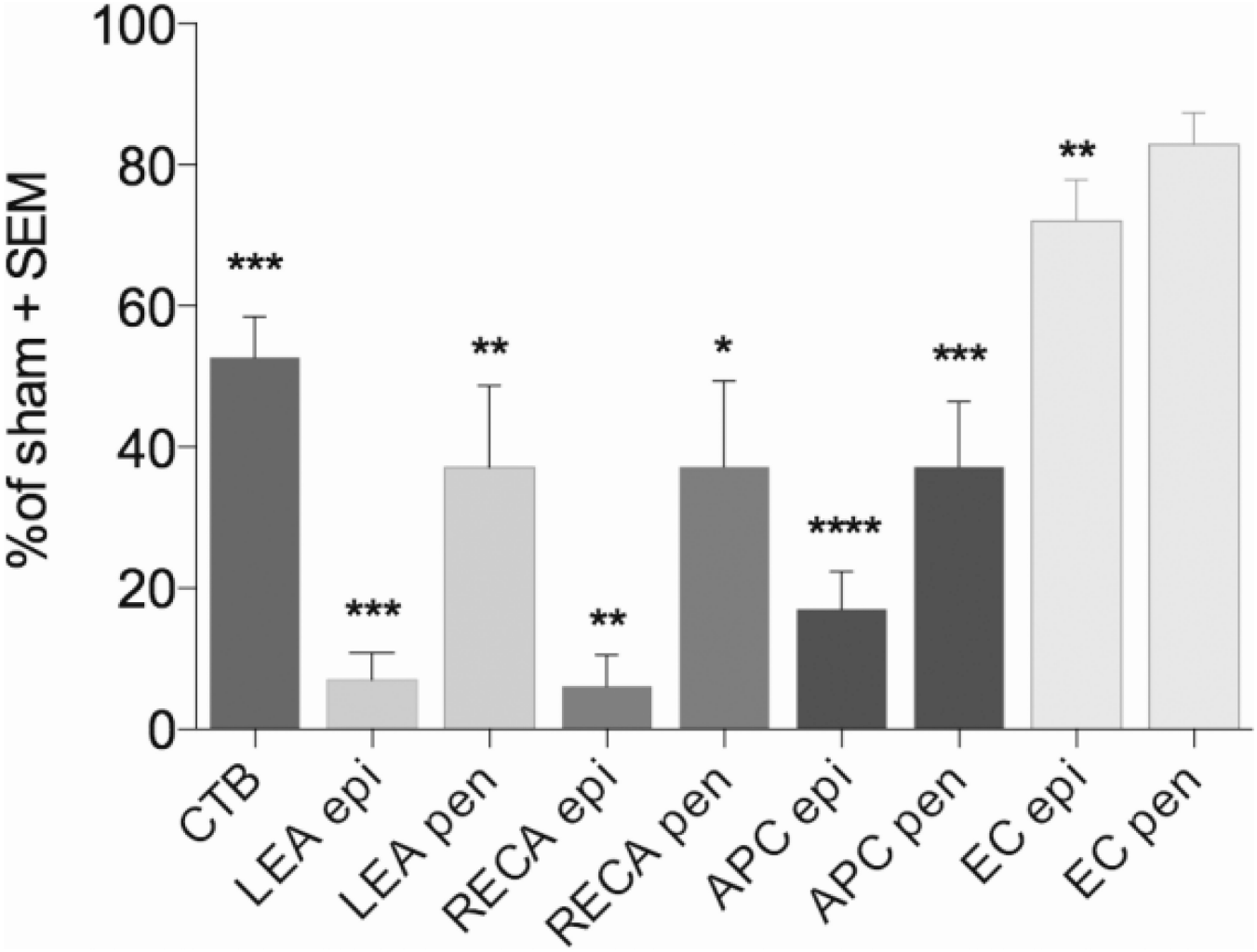

Figure 6. Quantification of axon, blood vessel, oligodendrocyte, and myelin loss 24 hours after phototoxic ischemia

The ischemic injury to the dorsal columns caused a loss of almost half of the sensory axons as assessed by CTB+ projections within the nucleus gracilis at 24 hours after the injury. Phototoxic ischemia also caused loss of total (RECA) and perfused (LEA) microvessels in the epicenter (epi) and penumbra (pen), confirming the success of the model. Ischemia also induced loss of APC+ oligodendrocytes in the epicenter and penumbra, as well as loss of myelin at the epicenter assess by EC staining. Sham, n = 4, ischemic injury n = 6. * $p < 0.05$, ** $p<0.01$, *** $p<0.001$,**** $p<0.0001$ compared to sham with one way ANOVA using Dunnett's multiple comparisons test.

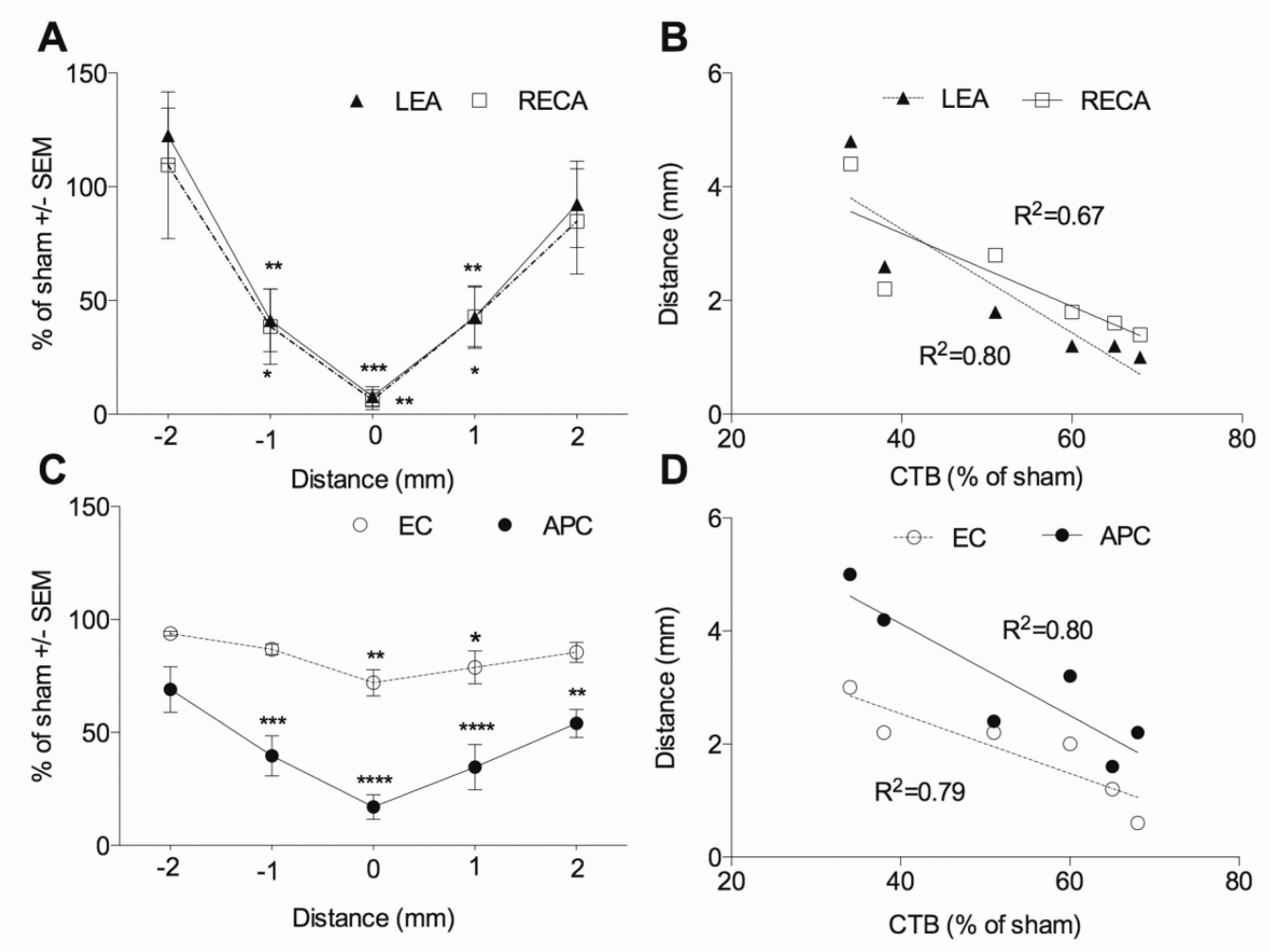

Figure 7. Dorsal column microvessel, oligodendrocyte, and myelin loss correlates with axon loss 24 hours after phototoxic ischemia

(**A**) Extensive loss of total (RECA) and perfused (LEA) microvessels was observed in the injury epicenter and at 1 mm away in the penumbra after focal phototoxic ischemia at T9. (**B**) The length of the microvessel loss (continuous area less than 33% of sham values) correlates negatively with dorsal column sensory axon sparing as assessed by CTB tracing of projections to the nucleus gracilis ($p < 0.05$). (**C**) Oligodendrocyte (APC) loss after phototoxic ischemia extends beyond the area of microvascular loss. Less severe loss of dorsal column myelin (EC) is observed in the epicenter and penumbra. (**D**) The length of oligodendrocyte and myelin loss (continuous area less than 33% of sham values) correlates negatively with dorsal column sensory axon sparing ($p < 0.05$). Sham, n = 4, ischemic injury, n = 6. *p<0.05; **p<0.01; ***p<0.001;, ****p<0.0001 compared with sham by two way ANOVA with Dunnett's multiple comparison's test).

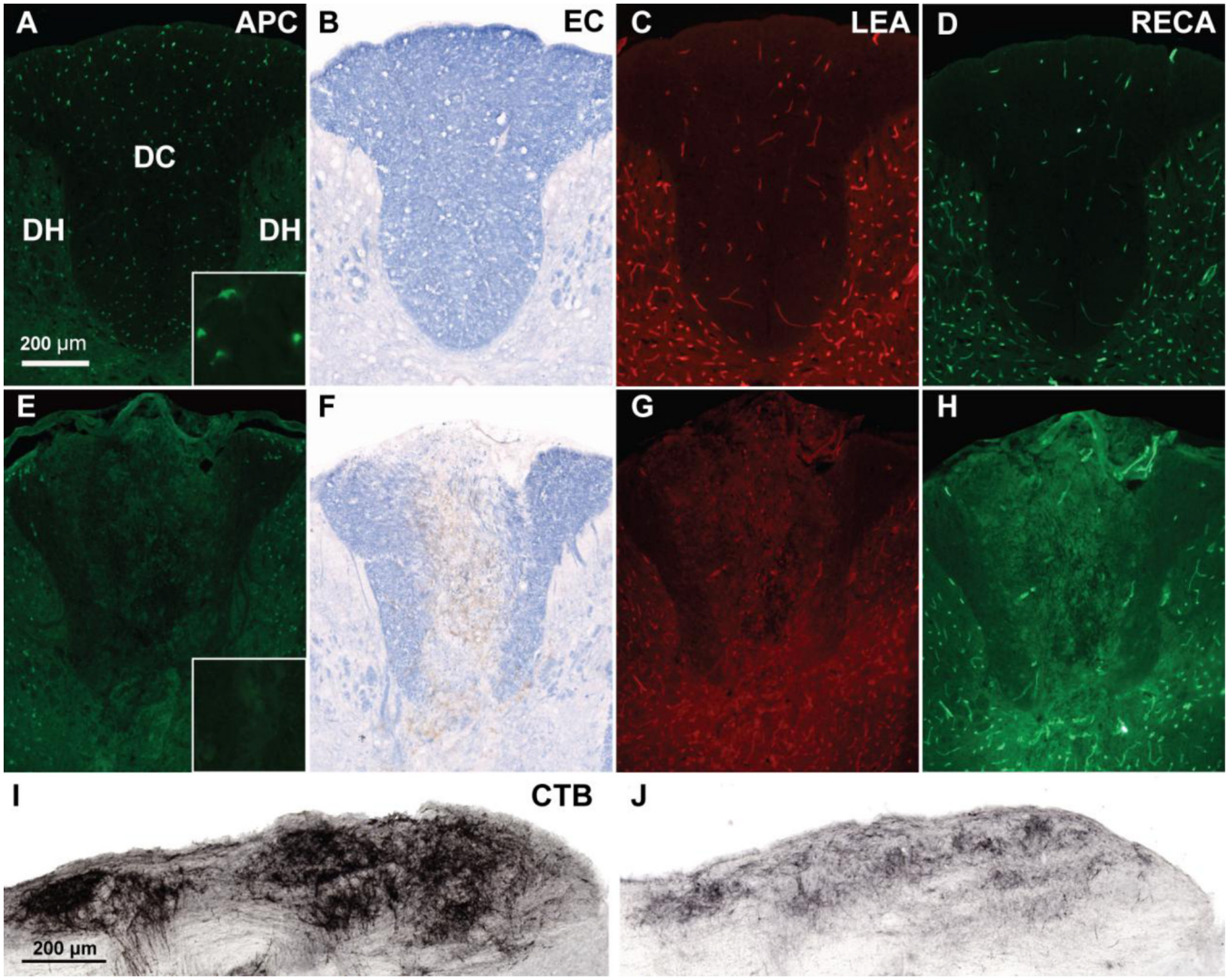

Figure 8. Dorsal column injection of 0.3 μg/μl EB causes oligodendrocyte, myelin, blood vessel, and sensory axon loss by 3 days

Compared to sham rats (**A**), rats injected with EB into two sites at T9 (**E**) had extensive loss of APC+ oligodendrocytes throughout the dorsal column. Demyelination of the dorsal column was also observed in EC stained sections in (**F**) compared to Sham (**B**). The injury was also accompanied with loss of total (RECA, **G**) and perfused (LEA, **H**) dorsal column microvessels when compared with Sham (**C,D**). Dorsal column sensory axon loss was observed in EB-injected rats, which had decreased anterogradely traced CTB+ projections in the nucleus gracilis (**J**) compared to sham rats (**I**). Scale bar = 200 μm. Insets in (A) and (E) show APC+ cell bodies taken with a 63× objective.

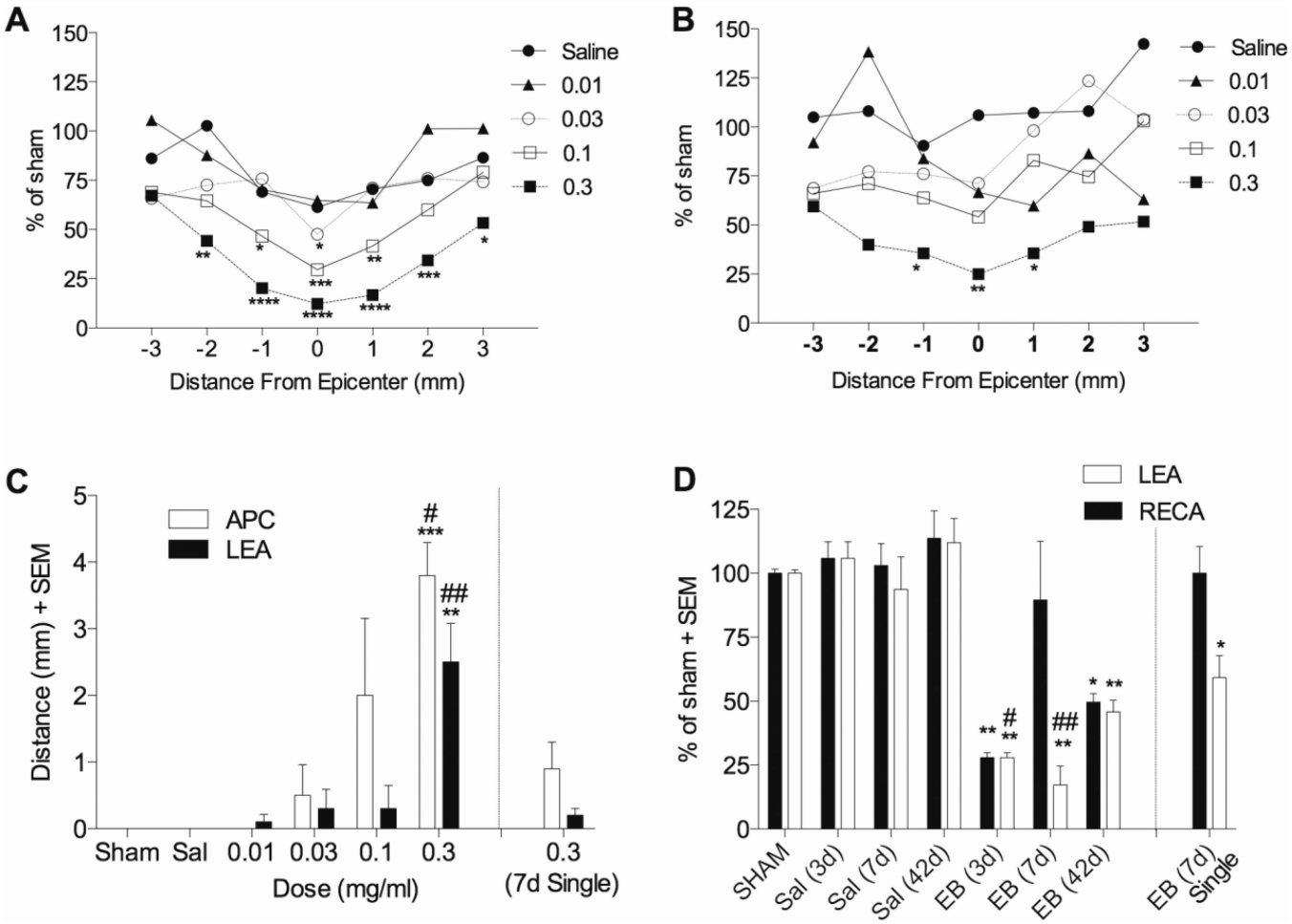

Figure 9. Dorsal column injection of EB induces oligodendrocyte and microvessel loss

(A) Oligodendrocyte (APC) and **(B)** microvessel (LEA) loss at 3 days after EB injection injected into the spinal cord shows the greatest loss at the epicenter occurring after 0.3 μg/μl (n=3 per group, except n=5 for 0.3 μg/μl EB). **(C)** Length of oligodendrocyte and microvessel loss, defined as the area in which microvessels or oligodendrocytes were less than 33% of sham values is significant only in rats receiving two injections of 0.3 μg/μl EB. **(D)** Microvessel loss at the epicenter occurs within 3 days after 0.3 μg/μl EB injection and remains decreased up to 42 days (n=3 for Sham, Sal 3d, and Sal 7d; n=6 for Sal 42d and EB42d; n=5 for EB 3d and EB 7d; n=4 for EB 7d (single)). *p<0.05; **p<0.01; ***p<0.001; ****p<0.0001 compared to sham by two way (**A, B**) or one way (**C, D**) ANOVA with Dunnett's multiple comparison's test. #p<0.05; ##p<0.01 compared to EB (7d) single injection by one way ANOVA with Tukey's multiple comparison's test.

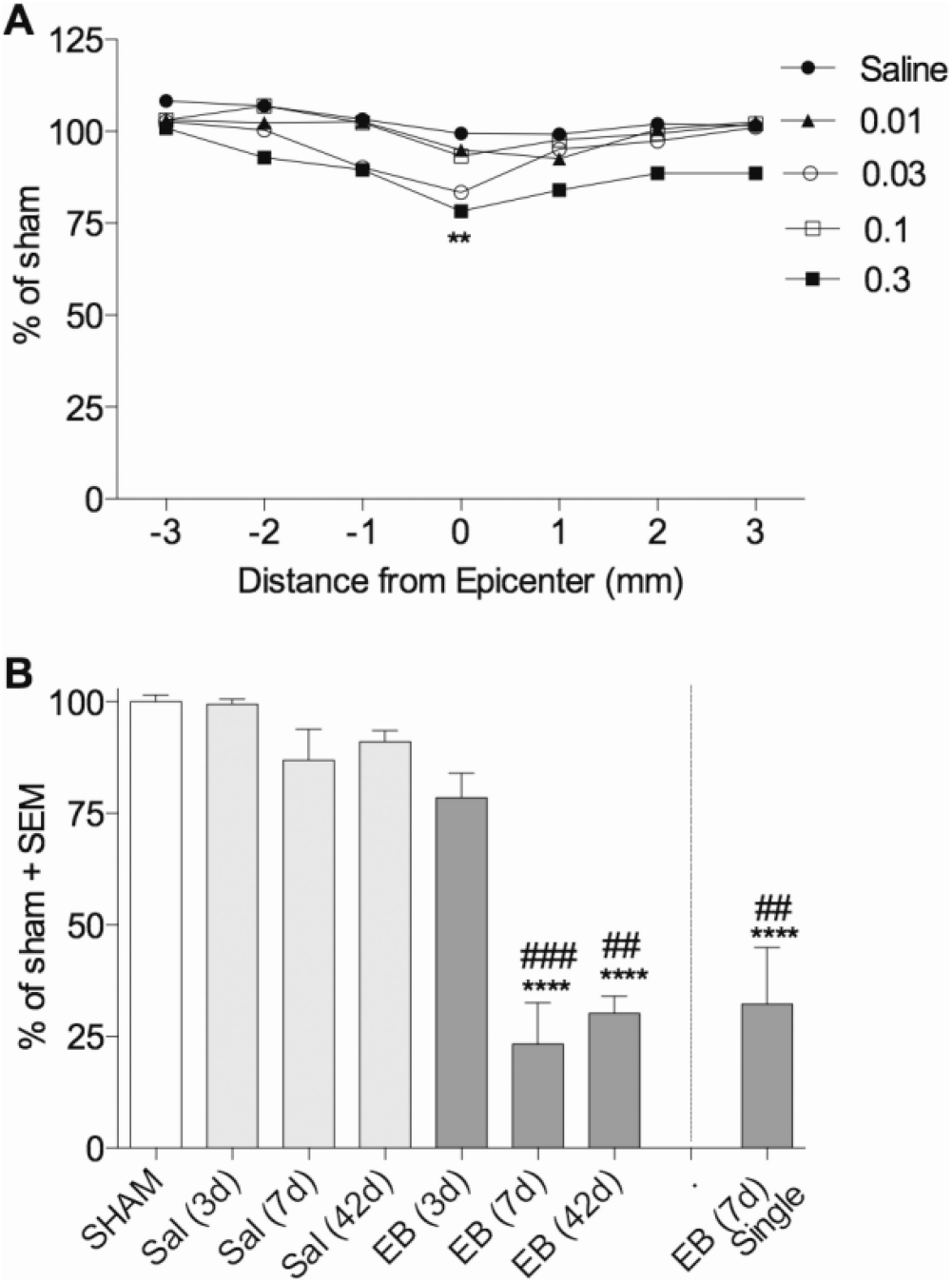

Figure 10. Dorsal column injection of EB causes progressive loss of myelin loss

(A) Only 0.3 μg/μl EB injected into the spinal cord at two sites T9 induced significant decreases in EC staining of dorsal column myelin 3 days after injection (n=3 per group, except n=5 for 0.3 0.3 μg/μl EB). **(B)** Peak myelin loss occurred by 7d after 0.3 μg/μl EB injection and remained low up to 42d (n=3 for Sham, Sal 3d, and Sal 7d; n=6 for Sal 42d and EB 42d; n=5 for EB 3d and EB 7d; n=4 for EB 7d (single). **p<0.01; ****p<0.0001 compared to sham by two way (A) or one way (B) ANOVA with Dunnett's multiple comparison's test. ##p<0.01; ###p<0.001 compared to EB (3d) by one way ANOVA with Tukey's multiple comparison's test.

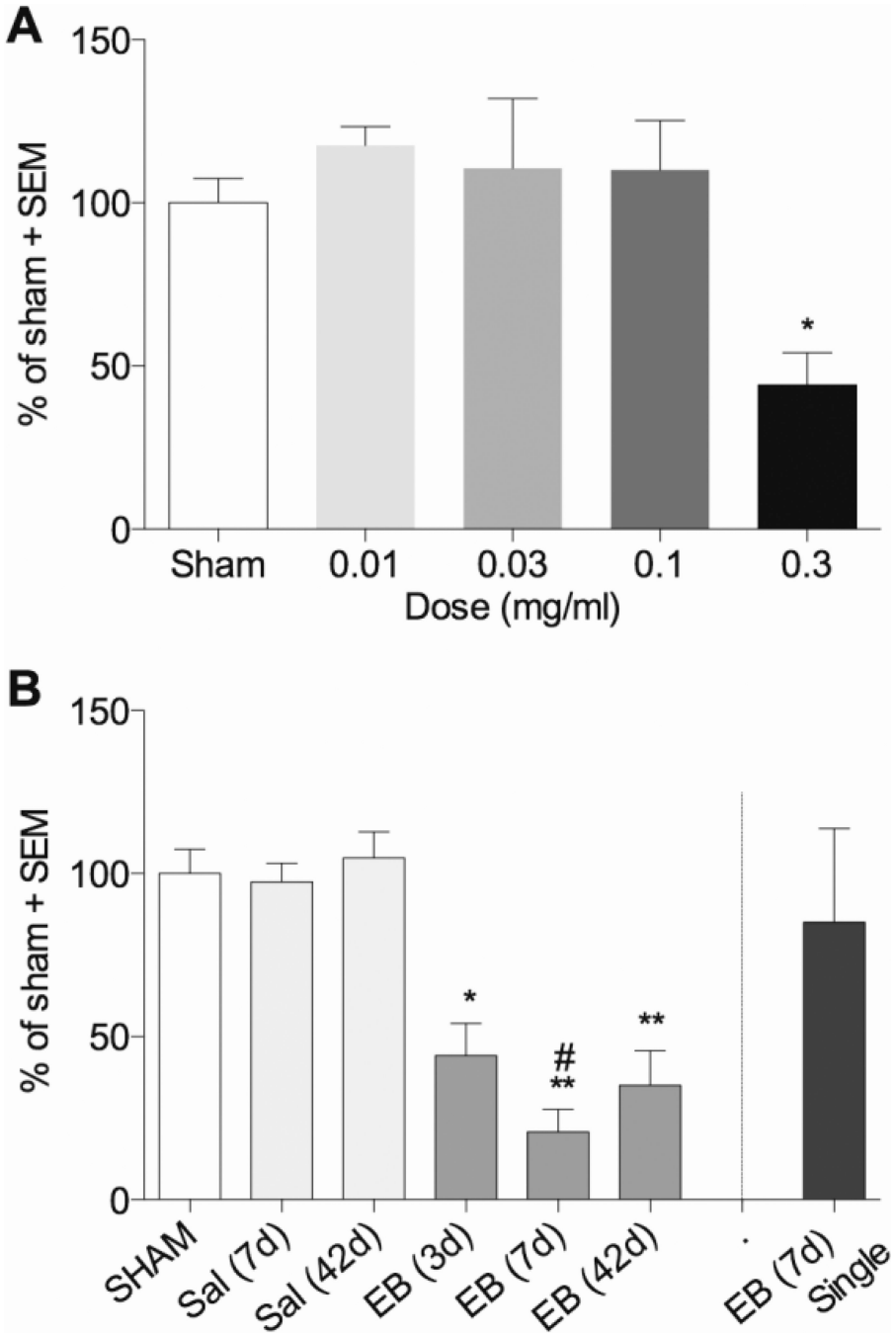

Figure 11. Local EB injection causes dorsal column sensory axon loss

(A) 3 days after two injections of EB (1.5 mm apart) at T9, the extent of CTB+ sensory axonal projections traced from the sciatic nerves to the nucleus gracilis was decreased only after 0.3 μg/μl EB (n=3 per group, except n=4 for Sham and n=2 for 0.03 μg/μl EB). **(B)** CTB+ values were decreased 3, 7 and 42 days after 0.3 μg/μl EB, but did not occur when only a single injection of EB was delivered (n=4 for sham and EB 7d; n=3 for Sal 7d and EB 3d; n= 5 for Sal 42d and EB 7d, n=6 for EB 42d). *p<0.05; **p<0.01; by one way ANOVA with Dunnett's multiple comparison's test. #p<0.05 compared to EB (7d) single injection by one way ANOVA with Tukey's multiple comparison's test.

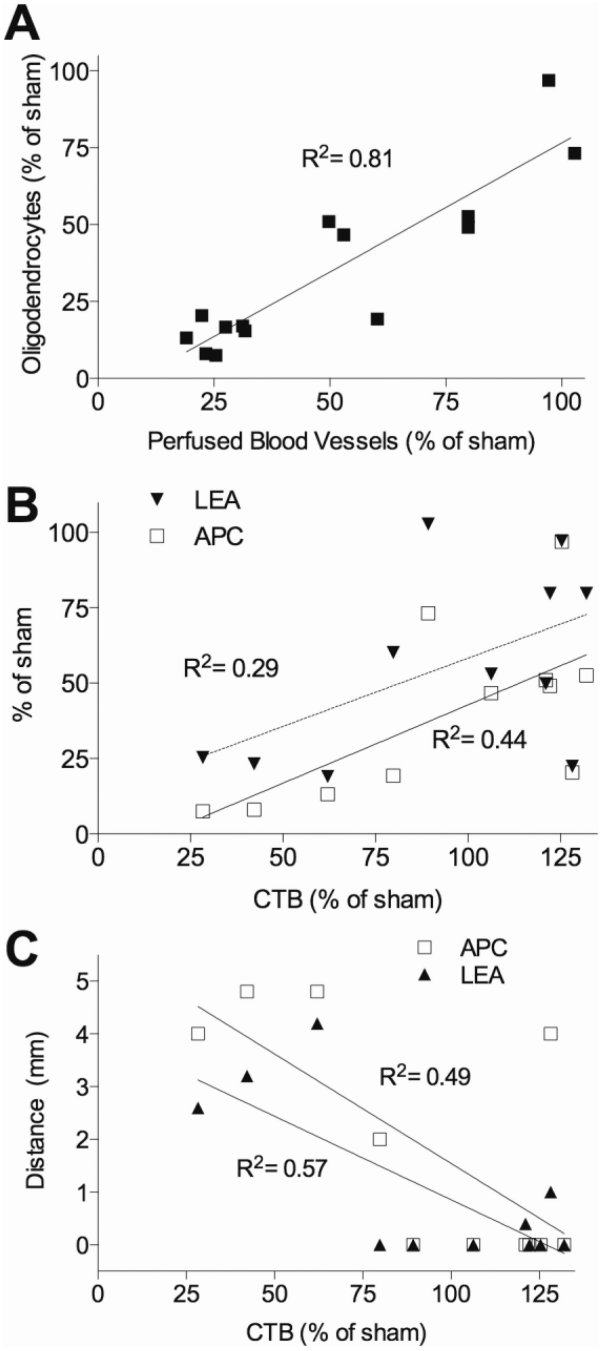

Figure 12. Sensory axon loss correlates with oligodendrocyte and microvessel loss after EB injury to the dorsal column

(A) Oligodendrocyte (APC) and blood vessel (LEA) loss is highly correlated 3 days after EB across all doses (0.01–0.3 μg/μl; n=14; $p < 0.0001$). **(B)** The degree of epicenter oligodendrocyte (APC) and blood vessel (LEA) loss correlates with sensory axon loss 3 days after EB (n=11; $p < 0.05$). **(C)** Length of oligodendrocyte and microvessel loss correlates negatively with sensory axon loss 3 days after EB (n=11; $p < 0.01$).

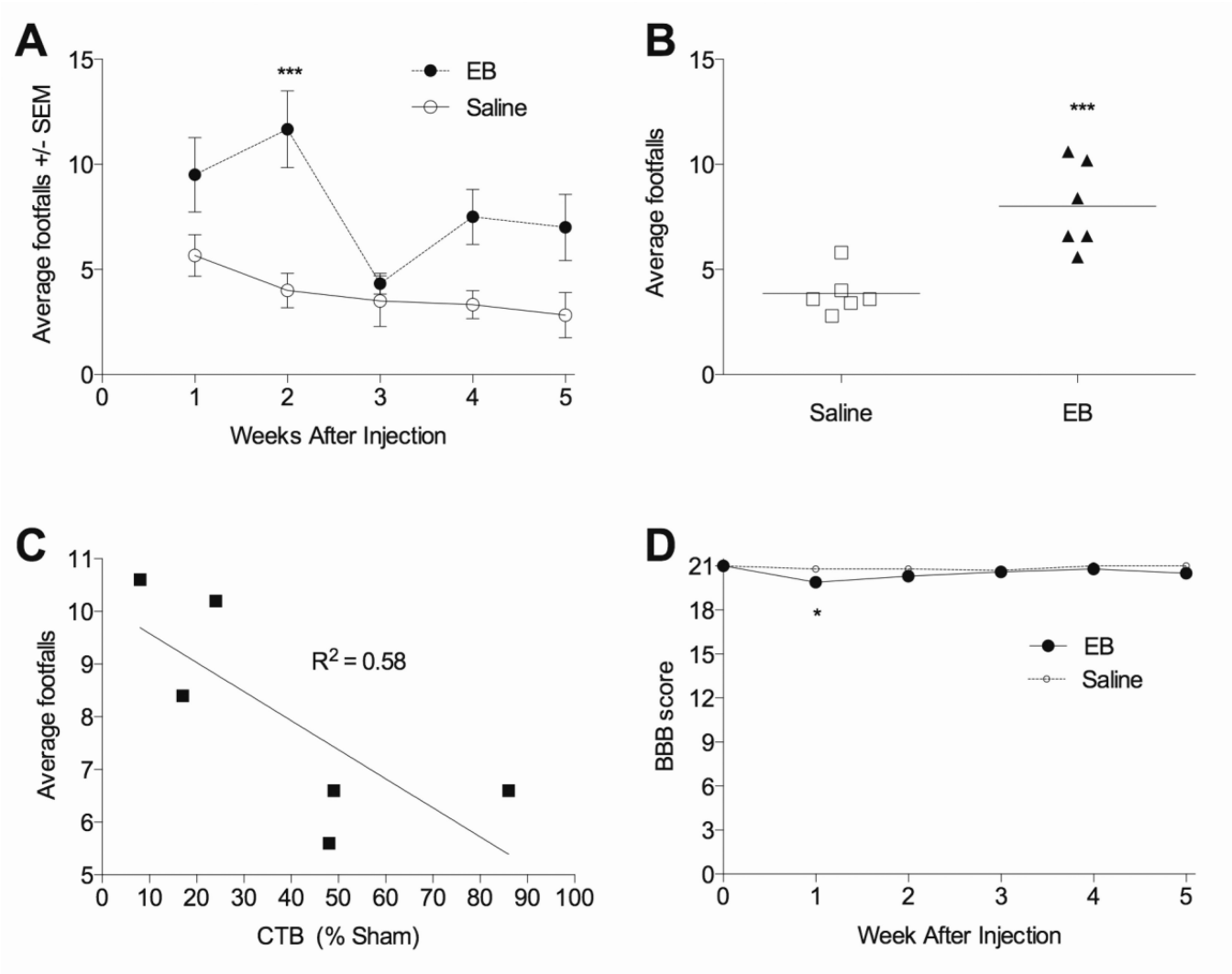

Figure 13. Functional deficits after EB injury to the dorsal columns

(A) Rats injected into the dorsal columns at T9 with two sites of 0.3 μg/μl EB made more hindlimb footfall errors during 90 seconds of grid walking two weeks after injection, most evident when footfall errors were averaged across weeks 1–5 **(B)**. **(C)** Within the 0.3 μg/μl EB treated group, the average number of footfalls from 1–5 weeks inversely correlated with the number of remaining ascending sensory dorsal column axons ($p < 0.05$). **(D)** Open field locomotion as assessed by the BBB test was unaffected by the dorsal column EB injury, though a very small, yet statistically significant difference was observed 1 week after injection. (**A–D**, n=6 group). *p<0.05; ***p<0.001 compared to saline by two way repeated measures ANOVA with Dunnett's multiple comparison's test (**A, D**) or by student's t-test (**C**).

Table 1

Number of rats per experiment

	Experiment	Groups and numbers	Total Number or rats
1	Developing a CTB tracing protocol to assess dorsal column sensory axons 24 hr post-injury	Sham 48 hours (n=7); sham 72 hours (n=9) 24 (n=5); 48 (n=4) or 7 days after contusion (n=6) and 24 hours after transection (n=5)	36
2	Temporal changes in microvessels and oligodendrocytes following 120 kdyn T9 contusion injury	Sham laminectomy vs. 3, 6 or 12 hours following injury (4/group)	16
3	Phototoxic injury at T9	Sham laminectomy (n=4); 24 hours after injury (n=6)	10
4	EB dose-effect study: 3 days post-injury	Sham (n=5), Saline (n=3), 0.01 (n=3), 0.03 (n=3), 0.1 (n=3), 0.3 (n=5) μg/μl EB	22
5	EB 7 day assessment	Saline (n=3), 0.3 μg/μl EB (n=9) (single and double injections)	12
6	EB Behavioral Study: 6 weeks plus motor function tests	Saline (n=6), 0.3 μg/μl EB (n=6)	12